DEVELOPMENT OF REACTION RATE EQUATIONS

The objective of this work is to develop a dependable rate expression for good plant design, rather than seeking to define the exact reaction mechanism. In this section, after a discussion on some considerations for kinetics studies, we will present analyses based upon both experience and theory. These analyses are —

- Analysis of Rate Expression
- Analysis of Carbon Formation
- Analysis of the Reversible Poisoning of Catalyst-Active Sites by Ammonia
- Analysis of Phenol Poisoning.

The following reactions may affect the water-gas shift reaction:

Group I

$$CO + H_2O \rightleftarrows CO_2 + H_2 \quad (11)$$

$$CO + 3H_2 \rightleftarrows CH_4 + H_2O \quad (12)$$

$$CO_2 + 4H_2 \rightleftarrows CH_4 + 2H_2O \quad (13)$$

$$C_2H_6 + 2H_2O \rightleftarrows 2CO + 5H_2 \quad (14)$$

$$C_2H_6 + 4H_2O \rightleftarrows 2CO_2 + 7H_2 \quad (15)$$

$$C_2H_6 + H_2 \rightleftarrows 2CH_4 \quad (16)$$

Group II

$$H_2S + CO \rightleftarrows COS + H_2 \quad (17)$$

$$H_2S + CO_2 \rightleftarrows COS + H_2O \quad (18)$$

$$H_2S + NH_3 \rightleftarrows NH_4HS \quad (19)$$

$$H_2S + 2NH_3 \rightleftarrows (NH_4)S \quad (20)$$

Group III

$$2CO \rightleftarrows CO_2 + C \quad (21)$$

$$CO_2 + 2H_2 \rightleftarrows 2H_2O + C \quad (22)$$

$$CO + H_2 \rightleftarrows H_2O + C \quad (23)$$

$$C_6H_6 \rightleftarrows 3H_2 + 6C \quad (24)$$

$$CH_4 \rightleftarrows 2H_2 + C \quad (25)$$

Group IV

$$2NH_3 \rightleftarrows N_2 + 3H_2 \quad (26)$$

$$C_6H_6 + H_2 \rightleftarrows \text{lower m.w. hydrocarbons} \quad (27)$$

$$C_6H_6 + C_6H_5OH + H_2O \rightleftarrows \text{alcohols, aldehydes} \quad (28)$$

Group I includes the water-gas shift, reforming, and hydrogenolysis reactions. Sulfided shift catalysts are poor methanation catalysts, and the ethane content of the feed was usually low. Therefore, water-gas shift is the primary reaction. An analysis of Reactions 11 and 12 was carried out and programmed. The equilibirum concentrations of the major components are presented in Figure 49.

Group II includes the reactions involving hydrogen sufide. Reactions 17 and 18 are significant, since they lead to carbonyl sulfide, which can present difficulties in later processing steps which remove sulfur compounds. Reactions 19 and 20 may explain the deactivation of the catalyst in the presence of ammonia when the sulfur content in the feed is low.

Group III includes the carbon formation reactions. This is an important group because carbon deposition is a serious process problem. It is discussed later in this report under a separate heading.

Group IV includes the possible decomposition of components that interfere with the water-gas shift reaction. Although we observed losses of these components during our studies, exact measurement was not obtained because of the very small amounts of these components in the feed mixtures. A more detailed study of these reactions could provide a better understanding of the behavior of the inhibition of the shift reaction and thus result in better process design capability.

Analysis of Rate Expression

One picture of the catalytic reaction involves the following assumptions:

a. All the reactions occur on the surface of the catalyst, and the catalyst surface has constant activity.

b. There is no interaction among adsorbed molecules except for the reaction of interest.

c. All the adsorption occurs by the same mechanism.

d. The extent of adsorption is less than one complete monomolecular layer on the surface.

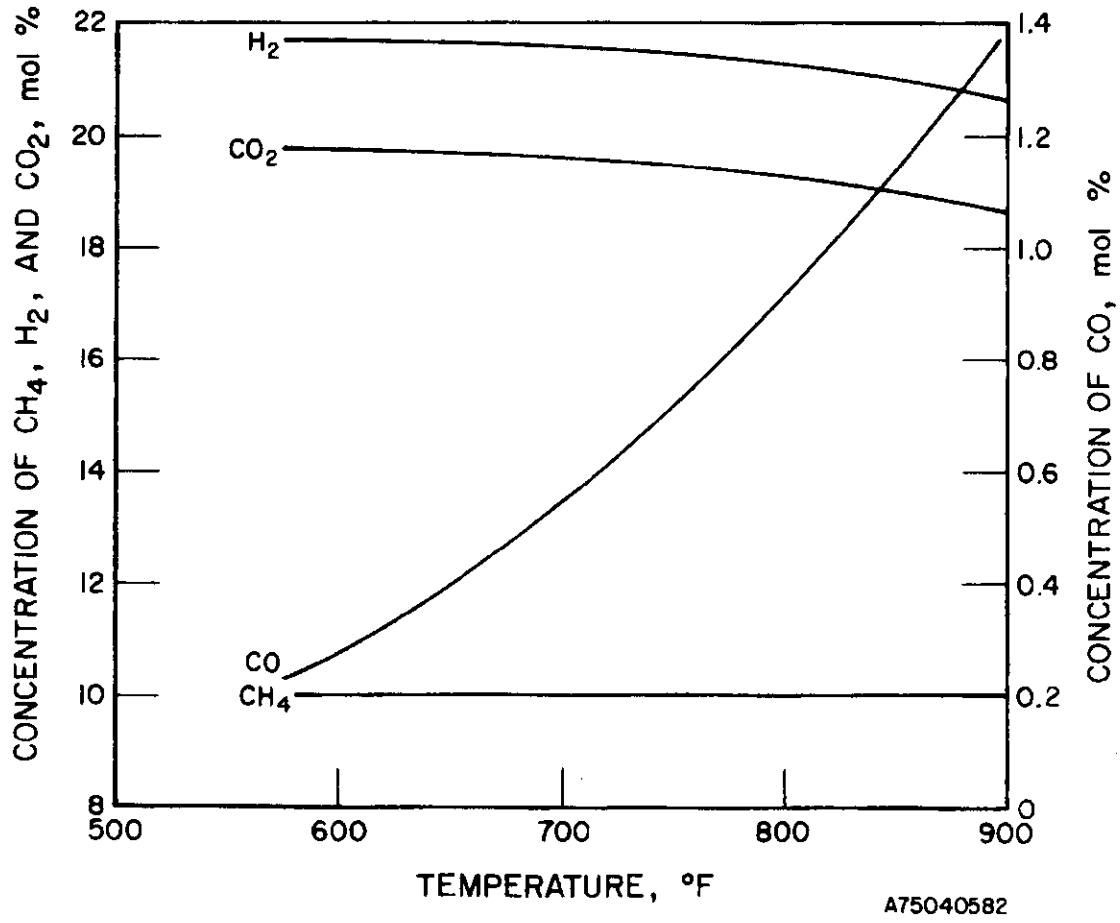

Figure 49. EQUILIBRIUM CONCENTRATION OF WATER-GAS SHIFT REACTION FOR A FEED CONCENTRATION OF 10% METHANE, 10% CARBON MONOXIDE, 12% HYDROGEN, 10% CARBON DIOXIDE, AND 58% WATER

In a system such as ours, where the reactants and products are gas phase and the catalyst is solid phase, the gas molecules are continually adsorbed on the solid surface, and some of these molecules later leave the surface. Equilibrium is established when the rate at which the molecules are adsorbed is exactly balanced by the rate at which they leave the surface.

For the water-gas shift reaction, let us simplify to the following form:

$$CO + H_2O \rightleftarrows \text{Products} \tag{29}$$

or

$$A + B \rightleftarrows C \tag{30}$$

In order to arrive at the overall Reaction 30, the individual steps are —

$A + X \rightleftarrows$	$A \cdot X$	Adsorption
$B + X \rightleftarrows$	$B \cdot X$	Adsorption
$A \cdot X + B \cdot X \rightleftarrows$	$C \cdot X + X$	Surface Reaction
$C \cdot X \rightleftarrows$	$C + X$	Desorption
$A + B \rightleftarrows$	C	Overall Reaction

where X represents a catalytic site on the surface.

The rate of adsorption is proportional to the concentration or pressure of the gas and the surface area that is available for adsorption. At a fixed temperature this is —

$$r_a = kp(1 - \varepsilon) \tag{31}$$

where —

k = proportional constant

ε = the fraction of surface already covered by adsorbed molecules

$1 - \varepsilon$ = the fraction of surface that is available for adsorption

p = pressure

and the rate of desorption is —

$$r_d = k'\varepsilon \tag{32}$$

At equilibrium, $r_a = r_d$, which leads to —

$$\varepsilon = \frac{kp}{k' + kp} = \frac{Kp}{1 + Kp} \tag{33}$$

where $K = k/k'$ is the adsorption equilibrium constant. Equation 33 is called the Langmuir Isotherm, and many rate expressions are derived from it.

Similar reasoning can be applied in more detail to suggest a form for the kinetic equation. Let —

C_a = the concentration of A in the gas phase

$\bar{C}$ = adsorbed concentration of all species on catalyst surface

$\bar{C}_m$ = concentration of a complete monomolecular layer.

Then the rate of adsorption is —

$$kC_a(\bar{C}_m - \bar{C}) \tag{34}$$

and the rate of desorption is $k'\bar{C}$.

At equilibrium, the two rates are equal, and —

$$\bar{C} = \frac{K\bar{C}_m C_a}{1 + KC_a} \tag{35}$$

The net rate of adsorption of component A is then —

$$r_a = kC_a(\bar{C}_m - \bar{C}) - k'\bar{C}_a = k[C_a(\bar{C}_m - \bar{C}) - \bar{C}_a/K_a] \tag{36}$$

where —

C_a = the concentration of A in the gas phase at the surface

$\bar{C}_a$ = the concentration of A adsorbed on the surface

K_a = adsorption equilibrium constant for A.

Let —

$\bar{C}_v = \bar{C}_m - \bar{C}$, the concentration of vacant sites.

Then, Equation 36 can be written as —

$$r_a = k(C_a \bar{C}_v - \bar{C}_a/K_a) \tag{37}$$

When the concentration of A on the catalyst is in equilibrium with that in the gas phase, the equilibrium concentration of A, $(\bar{C}_a)_{equil}$, may be expressed as —

$$(\bar{C}_a)_{equil} = K_a C_a \bar{C}_v \tag{38}$$

For the surface reaction portion of Reaction 30, the forward reaction is —

INSTITUTE OF

$$k_s \bar{C}_a \bar{C}_b / \bar{C}_m \quad (39)$$

where —

$\bar{C}_a$ = the concentration of A absorbed on the surface

$\bar{C}_b$ = the concentration of B absorbed on the surface

$\bar{C}_m$ = the total molal concentration of active sites

so that —

$\bar{C}_b/\bar{C}_m$ = the fraction of the sites adjacent to A occupied by B, or the fraction of the total surface occupied by B.

The reverse rate is then —

$$k_s' \bar{C}_c \bar{C}_v / \bar{C}_m \quad (40)$$

and the net surface rate is —

$$r_s = (k_s \bar{C}_a \bar{C}_b - k_s' \bar{C}_c \bar{C}_v)/\bar{C}_m = (\bar{C}_a \bar{C}_b - \bar{C}_c \bar{C}_v / K_s)/\bar{C}_m \quad (41)$$

where K_s is the equilibrium constant for the surface reaction.

For the desorption of C, the rate is —

$$r_d = k_d' \bar{C}_c - k_d C_c \bar{C}_v = -k_d (C_c \bar{C}_v - \bar{C}_c / K_c) \quad (42)$$

To express the rate in terms of quantities that can be measured experimentally, all the surface concentration terms, $\bar{C}_i$, must be eliminated. Assuming that the rate is surface-reaction-controlling, all the adsorption and desorption concentration will be at equilibrium, and we may write equations similar to Equation 38:

$$(\bar{C}_b)_{equil} = K_b C_b \bar{C}_v \quad (43)$$

and

$$(\bar{C}_c)_{equil} = K_c C_c \bar{C}_v \quad (44)$$

Substituting into Equation 41, we have —

$$r_s = (K_a K_b C_a C_b \bar{C}_v^2 - C_c \bar{C}_v^2 / k_s) C_m \quad (45)$$

and $\bar{C}_v$, the concentration of vacant sites, can be expressed in terms of the total concentration of sites, $\bar{C}_m$, as —

$$\bar{C}_m = \bar{C}_a + \bar{C}_b + \bar{C}_c + \bar{C}_v \quad (46)$$

Because we are assuming equilibrium values for $\bar{C}_a$, $\bar{C}_b$, and $\bar{C}_c$, Equations 38, 43, 44, and 46 are combined to give —

$$\bar{C}_v = \bar{C}_m/(1 + K_a C_a + K_b C_b + K_c C_c) \tag{47}$$

Substituting into Equation 45 —

$$r_s = k_s \bar{C}_m \frac{K_a K_b C_a C_b - (K_c/K_s) C_c}{(1 + K_a C_a + K_b C_b + K_c C_c)^2} \tag{48}$$

Equation 48 can be simplified by substituting the conventional equilibrium constant for the reaction —

$$K = (C_c/C_a C_b)_{equil} = \frac{\bar{C}_c/K_c \bar{C}_v}{(\bar{C}_a/K_a \bar{C}_v)(\bar{C}_b/K_b \bar{C}_v)}$$
$$= \frac{K_a K_b}{K_c} \left(\frac{\bar{C}_v \bar{C}_c}{\bar{C}_a \bar{C}_b} \right)_{equil} = K_a K_b K_s/K_c \tag{49}$$

and Equation 48 becomes

$$r_s = k_s \bar{C}_m K_a K_b \frac{C_a C_b - C_c/K}{(1 + K_a C_a + K_b C_b + K_c C_c)^2} \tag{50}$$

A similar technique may be used for the other two possible rate-controlling steps, adsorption and desorption, and the rate equations developed will have approximately the same form. The actual rate analysis of a process is usually much more complex than this. There are usually more than three components and more than one reaction occurring, and the reaction order of each component is not always equal to 1. Obviously, the effectiveness of a rate equation, such as Equation 50, depends upon the appropriateness of the values of the constants k_s, $\bar{C}_m$, K_a, K_b, K_c, and K. Determining these values from theory is not practical, and we have followed the procedure of deriving them, except K, from experimental kinetics data. Thus, the form of the rate equation is based on theory, but the values of the constants are based on the experimental data. The importance of the method chosen and precision of the kinetics data cannot be overemphasized. The applicability of the final rate expression is only as good as these data. Therefore, we have minimized the reaction variables. All terms in Equation 50 are extremely sensitive to temperature and, therefore, isothermal data are essential. We can see that composition is as important as temperature, and it is necessary to minimize composition gradients during each experiment. All components may hinder or

assist the rate of reaction; therefore, the experimental program must include all species that are present in an actual plant. If the reaction is diffusion-controlled, as it is in this case, the rate is also a function of the physical properties of the catalyst – surface area, pore size, pore volume, etc.

We must also take the realities of process engineering into consideration. The study was made on the same catalyst particle size that will be used in the plant. The performance of different catalysts and that of different particle sizes of the same catalyst may not be identical. It could be very misleading to study the catalyst in micron size in the laboratory and then scale it up to commercial-plant-size operation.

Rate Equation Based on the Experimental Data for the G-93 Catalyst

The water-gas shift reaction will not proceed at a significant rate in the absence of a catalyst for the conditions studied here. Therefore, it can be safely concluded that the rate is a function of the adsorption process, the surface reaction process, the desorption process, or some combination of these. Regardless of which step is considered to be rate-controlling, the final rate equation will have the following:

$$r = \frac{kC_1^{a}\,C_2^{b}\cdots}{1 + (K_iC_1 + K_jC_2 + K_mC_3\cdots)^{y}} \qquad (51)$$

As examples, in the case of a reaction rate controlled by the adsorption step, the rate equation is of the form –

$$r = \frac{k\bar{C}_m[C_a - (1/K)(C_c/C_b)]}{1 + K_cC_b + (K_a/K)(C_c/C_b) + K_cC_c} \qquad (52)$$

In the case of surface-reaction-controlled rates, the rate equation is –

$$r = kC_m\,K_aK_b\,\frac{C_aC_b - (1/K)C_c}{(1 + K_aC_a + K_bC_b + K_cC_c)^2} \qquad (53)$$

In desorption-controlled rates –

$$r = kC_mK\,\frac{C_aC_b - (1/K)C_c}{1 + K_aC_a + K_bC_b + K_cKC_aC_b} \qquad (54)$$

Following the form of these equations, the following rate expression was determined from the experimental data for the G-93 catalyst:

$$r = \frac{kP_{CO}^{0.5}\,P_{H_2O}^{0.25}}{1 + 0.002P_{H_2O} + 0.01P_{C_6H_6}} \qquad (55)$$

where —

r = rate of carbon monoxide conversion X 10^{-4} lb-mol/hr-g catalyst

P_{CO} = partial pressure of carbon monoxide, psig

P_{H_2O} = partial pressure of water, psig

$P_{C_6H_6}$ = partial pressure of benzene, psig

k = rate constant = $k_o \exp(-E/RT)$

k_o = 0.35

E = 4194 Btu/lb-mol (2.3 kcal/g-mole)

R = 1.987 Btu/lb-mol-°R

T = temperature, °R.

Equation 55 is applicable for the following 11 conditions:

1. Temperatures ranging from the dew point of the feed gas to 750°F
2. Pressures from 200 to 1000 psig
3. Steam/gas mole ratios of 0.5 or larger
4. Steam/benzene mole ratios of 6.0 or larger
5. Benzene concentrations in the feed less than 20 mole %
6. Inert gas (nitrogen, helium) concentrations in the feed less than 5 mole %
7. Hydrocarbons of C_2^+ concentrations in the feed less than 5 mole %
8. Carbon monoxide concentrations in the feed less than 30 mole %
9. Sulfur concentrations in the feed more than 1 mole %
10. Ammonia concentrations in the feed less than 1 mole %
11. No phenol present. (Phenol is a poison and is considered a side-by-side reaction to the water-gas shift reaction. This poisoning effect is discussed later.)

All the concentrations mentioned above are on a water-free basis.

The exponents, or reaction orders in Equation 55, were determined graphically from log-log plots of the rate data, as shown in Figures 50 and 51.

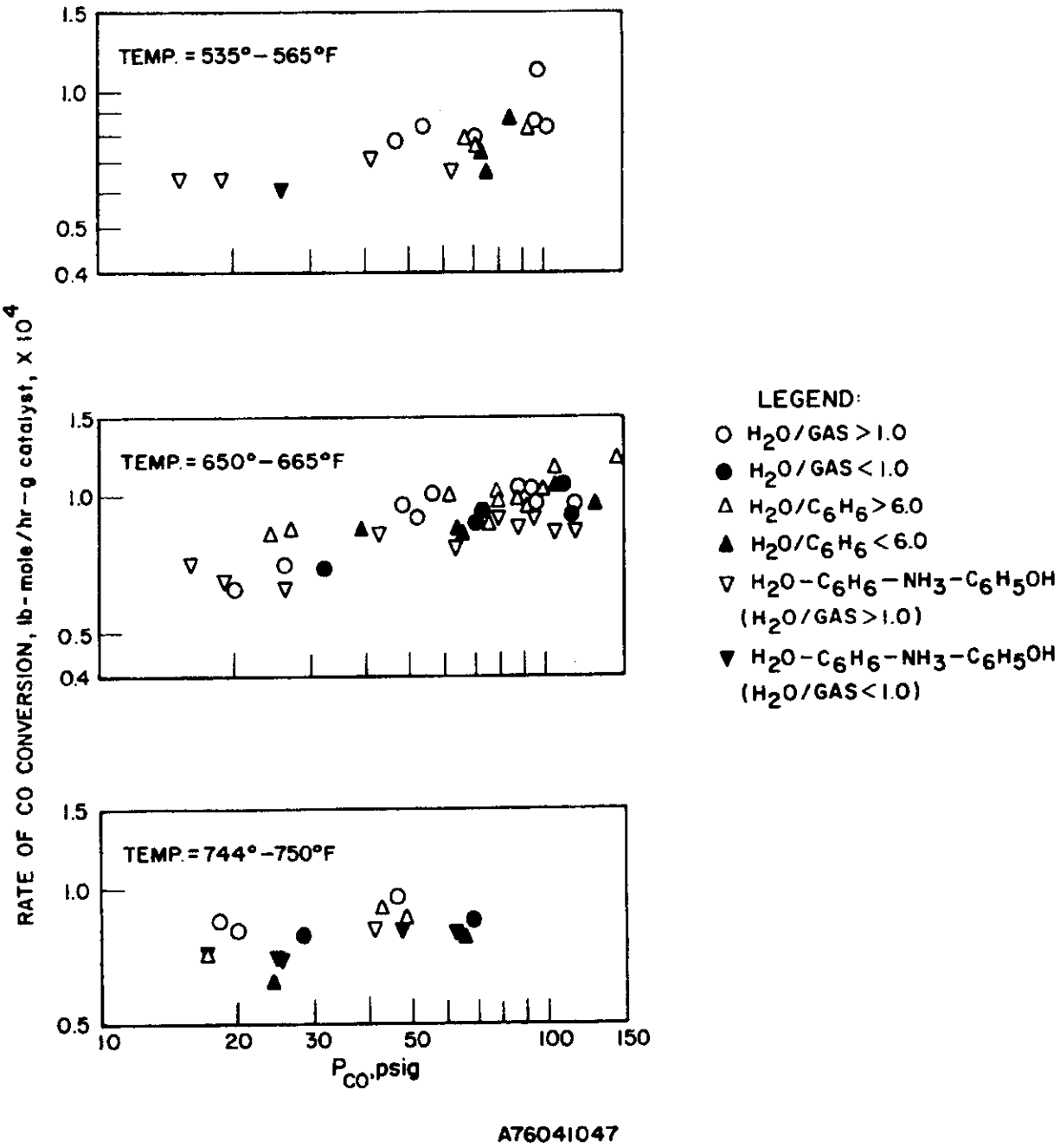

Figure 50. GRAPHICAL REPRESENTATION OF THE REACTION ORDER OF CARBON MONOXIDE IN THE WATER-GAS SHIFT REACTION (Girdler G-93 Catalyst, 4 x 6 Mesh Spheres)

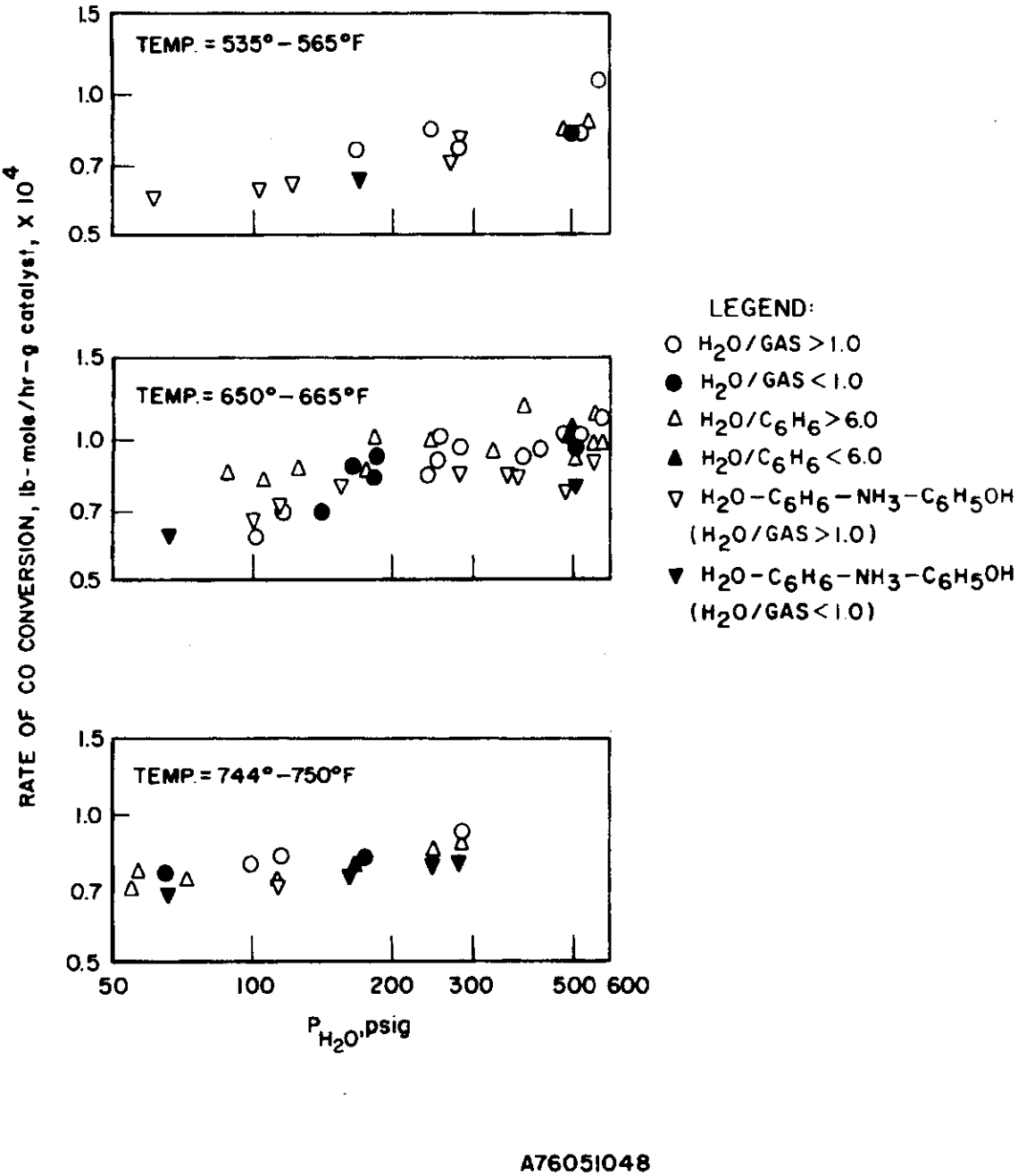

Figure 51. GRAPHICAL REPRESENTATION OF THE REACTION ORDER OF WATER IN THE WATER-GAS SHIFT REACTION (Girdler G-93 Catalyst, 4 x 6 Mesh Spheres)

The behavior of the water-gas shift reaction is summarized in Figure 52, which shows nine sets of data. Excess benzene or low water/benzene ratios retard the rate of reaction as well as promote carbon formation reactions. Phenol poisons the catalyst, and methane and carbon dioxide have zero reaction orders.

The temperature dependence of this reaction is shown in Figure 53, a standard Arrhenius plot, and was used in the determination of the rate constant.

Rate Equation Based on Experimental Data for the UC-1870-46-1 Catalyst

The rate data for this catalyst were compared with the data obtained with the G-93 catalyst and are presented in Figures 54 through 57. We observed that —

- Higher conversions of carbon monoxide were obtained for all pressures with this catalyst than with the G-93 catalyst (Figures 54 through 56).
- The presence of benzene in the feed retarded carbon monoxide conversion and promoted carbon formation (Figure 57).
- The carbon monoxide conversion was not linearly proportional to pressure (Figures 54 through 56), nor was the rate of carbon monoxide conversion (Figure 58).
- The range of carbon formation using this catalyst was greater than that using the G-93 catalyst (Figure 59).
- A high concentration of phenol (0.4 mole %) in the feed promoted carbon formation.
- A distinct pattern of pressure dependence, particularly below 200 psig.

To examine the effect of pressure in more detail, we assumed that the gaseous reactants and products behave as ideal gases, and then substituted —

$$C_i = p_i/R_gT \tag{56}$$

into the rate Equations 52, 53, and 54.* At zero conversion, the pressure of the products is zero and, for an equimolal mixture, we have —

$$P_A = P_B = 1/2p_t \tag{57}$$

For the adsorption controlling case and at initial conditions, by combining constants we obtain —

* Presented in a preceding section entitled "Rate Equations Based on the Experimental Data Using the G-93 Catalyst."

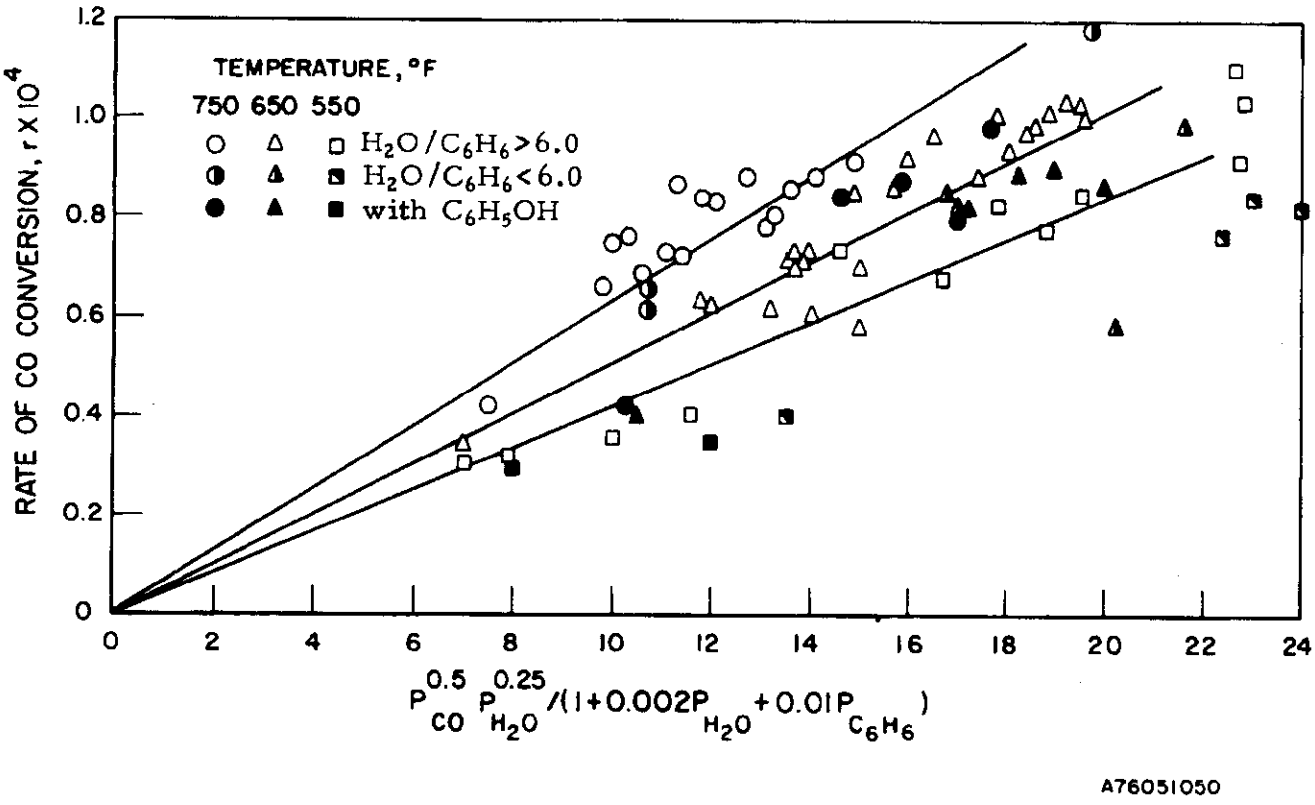

Figure 52. DETERMINATION OF THE RATE CONSTANT FOR THE WATER-GAS SHIFT REACTION (G-93 Catalyst)

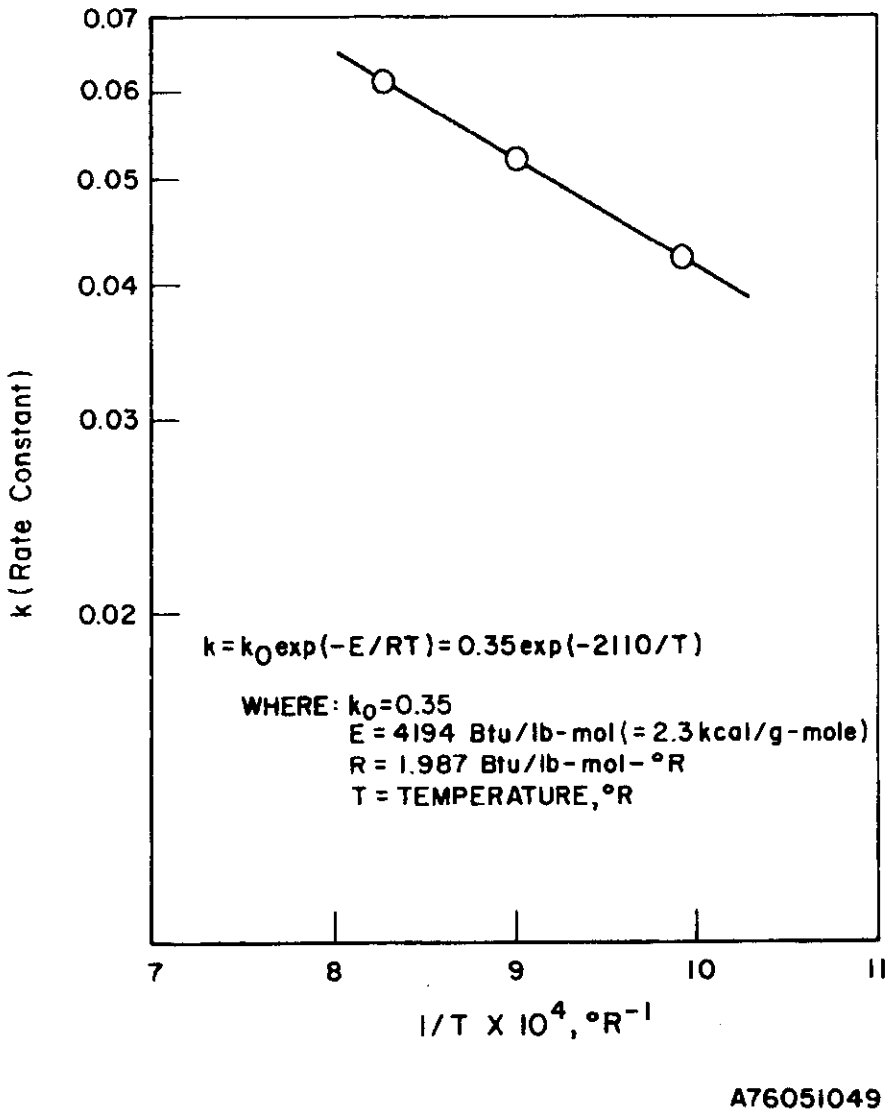

Figure 53. ARRHENIUS PLOT FOR THE WATER-GAS SHIFT REACTION BASED ON THE RATE EQUATION (G-93 Catalyst)

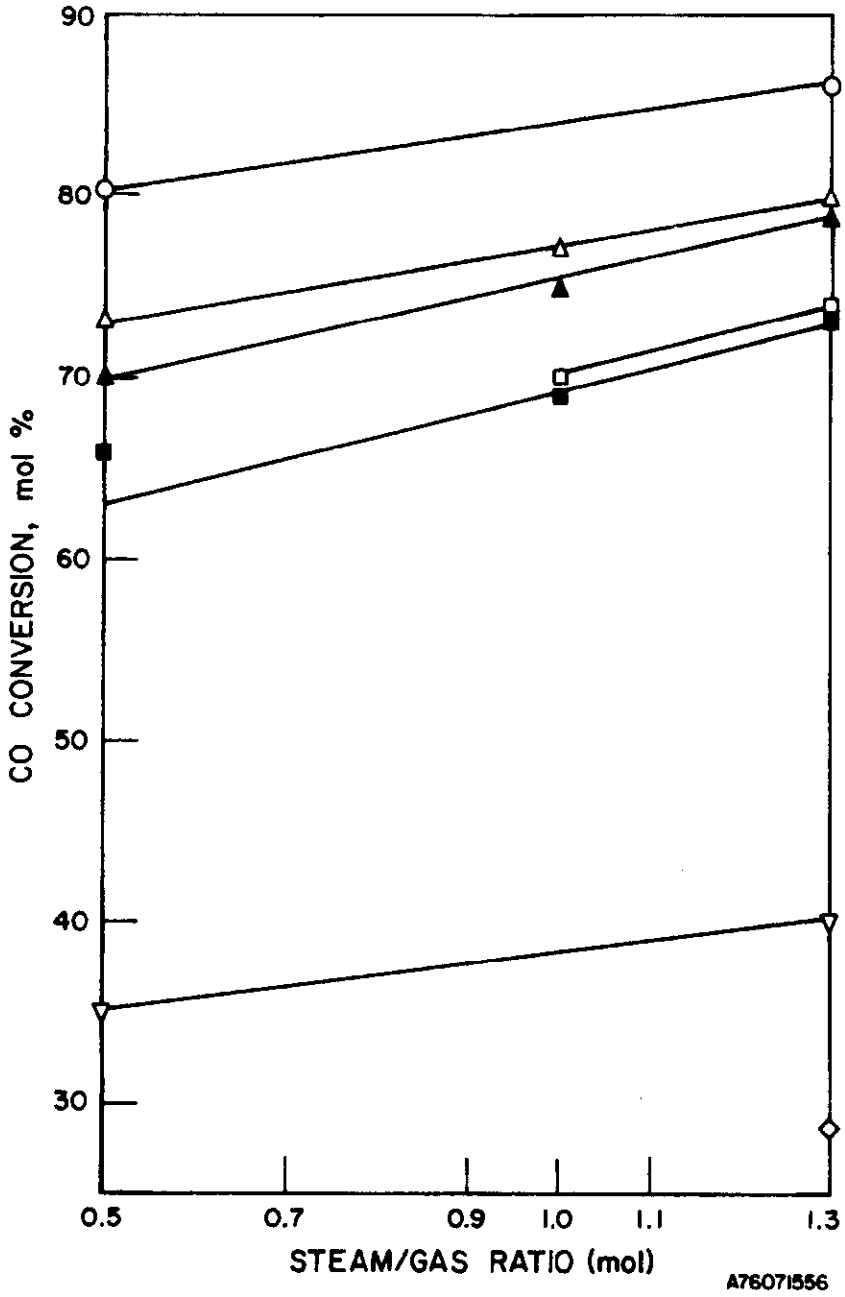

CATALYST UC	CATALYST G-93	PRESSURE, psig
○	●	1000
△	▲	500
□	■	200
▽	▼	100
◇	◆	50

FEED GAS COMPOSITION, dry basis

COMPONENT	mol %
CO	13.2
CO_2	16.4
H_2	37.5
CH_4	27.18
C_2H_6	1.1
C_3H_8	0.8
C_4H_{10}	0.1
H_2S	2.4
N_2	1.2
He	0.02
NH_3	0
C_6H_5OH	0
C_6H_6	0
COS	0.1
CH_3SH ppm	--
C_3H_7SH ppm	1.6
C_4H_4S ppm	0.8
TOTAL	100.00

Figure 54. EFFECT OF STEAM/GAS RATIO ON CONVERSION OF CARBON MONOXIDE (At 745° to 755°F and a CSTR Space Velocity of 0.2230 SCF/hr-g)

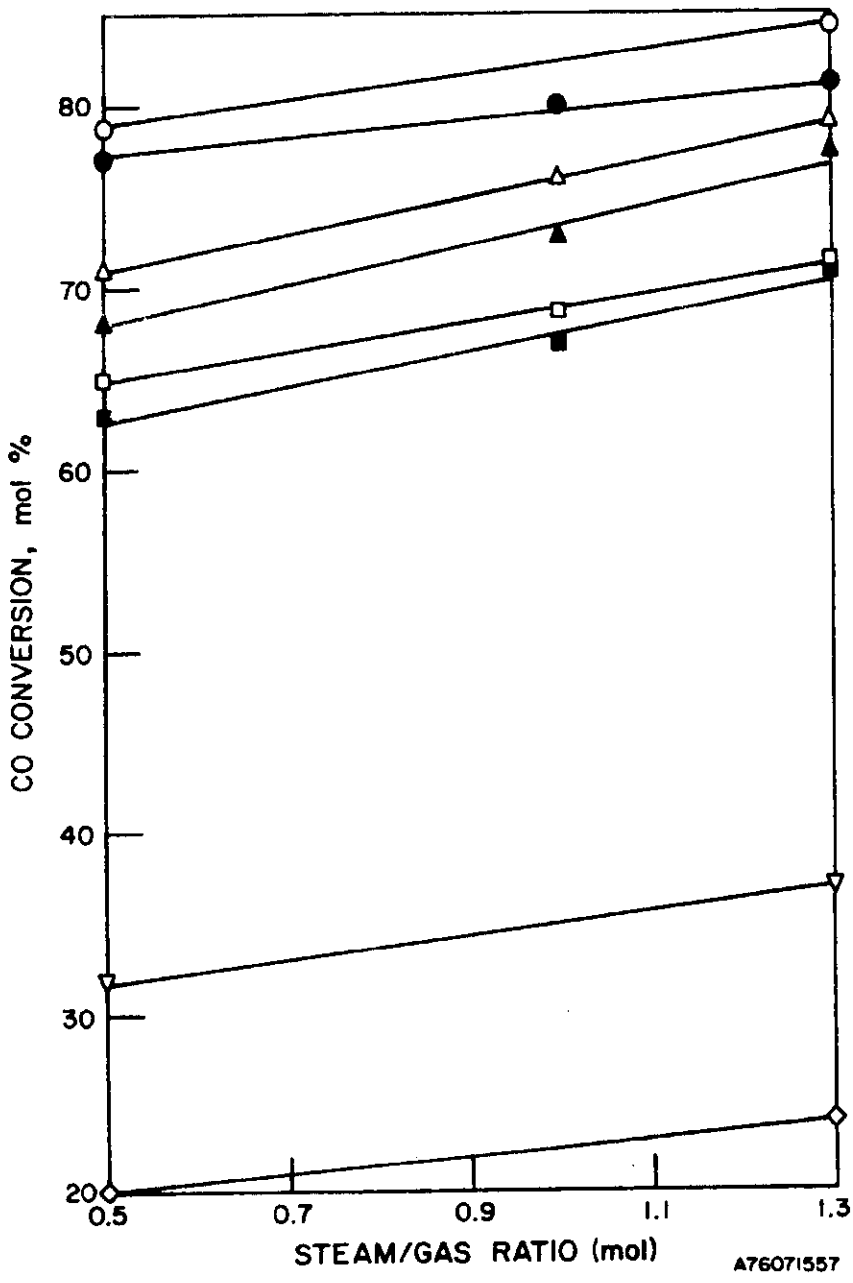

CATALYST UC	CATALYST G-93	PRESSURE, psig
○	●	1000
△	▲	500
□	■	200
▽	▼	100
◇	◆	50

FEED GAS COMPOSITION, dry basis

COMPONENT	mol %
CO	13.2
CO_2	16.4
H_2	37.5
CH_4	27.18
C_2H_6	1.1
C_3H_8	0.8
C_4H_{10}	0.1
H_2S	2.4
N_2	1.2
He	0.02
NH_3	0
C_6H_5OH	0
C_6H_6	0
COS	0.1
CH_3SH ppm	--
C_3H_7SH ppm	1.6
C_4H_4S ppm	0.8
TOTAL	100.00

Figure 55. EFFECT OF STEAM/GAS RATIO ON CONVERSION OF CARBON MONOXIDE
(At 650° to 660°F and a CSTR Space Velocity of 0.2230 SCF/hr-g)

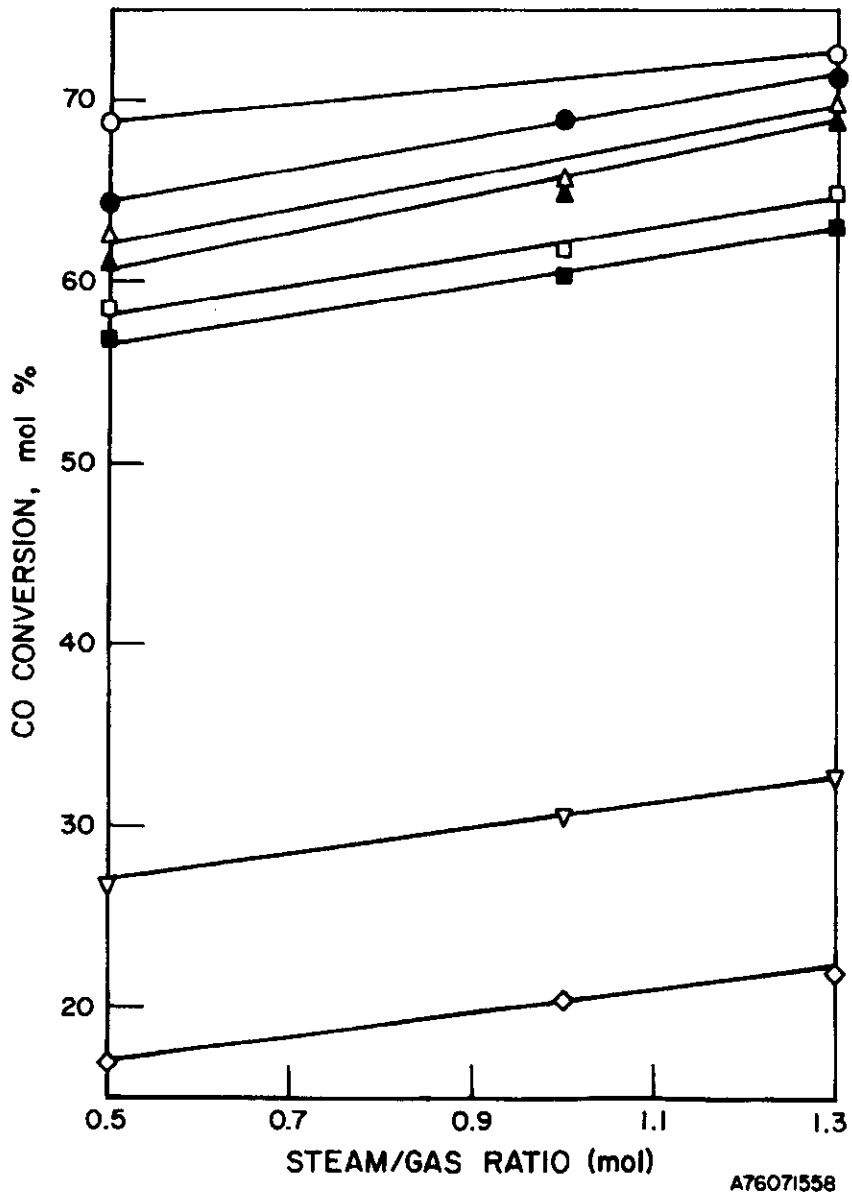

CATALYST UC	CATALYST G-93	PRESSURE, psig
○	●	1000
△	▲	500
□	■	200
▽	▼	100
◇	◆	50

FEED GAS COMPOSITION, dry basis

COMPONENT	mol %
CO	13.2
CO_2	16.4
H_2	37.5
CH_4	27.18
C_2H_6	1.1
C_3H_8	0.8
C_4H_{10}	0.1
H_2S	2.4
N_2	1.2
He	0.02
NH_3	0
C_6H_5OH	0
C_6H_6	0
COS	0.1
CH_3SH ppm	--
C_3H_7SH ppm	1.6
C_4H_4S ppm	0.8
TOTAL	100.00

Figure 56. EFFECT OF STEAM/GAS RATIO ON CONVERSION OF CARBON MONOXIDE (At 550° to 560°F and a CSTR Space Velocity of 0.2230 SCF/hr-g)

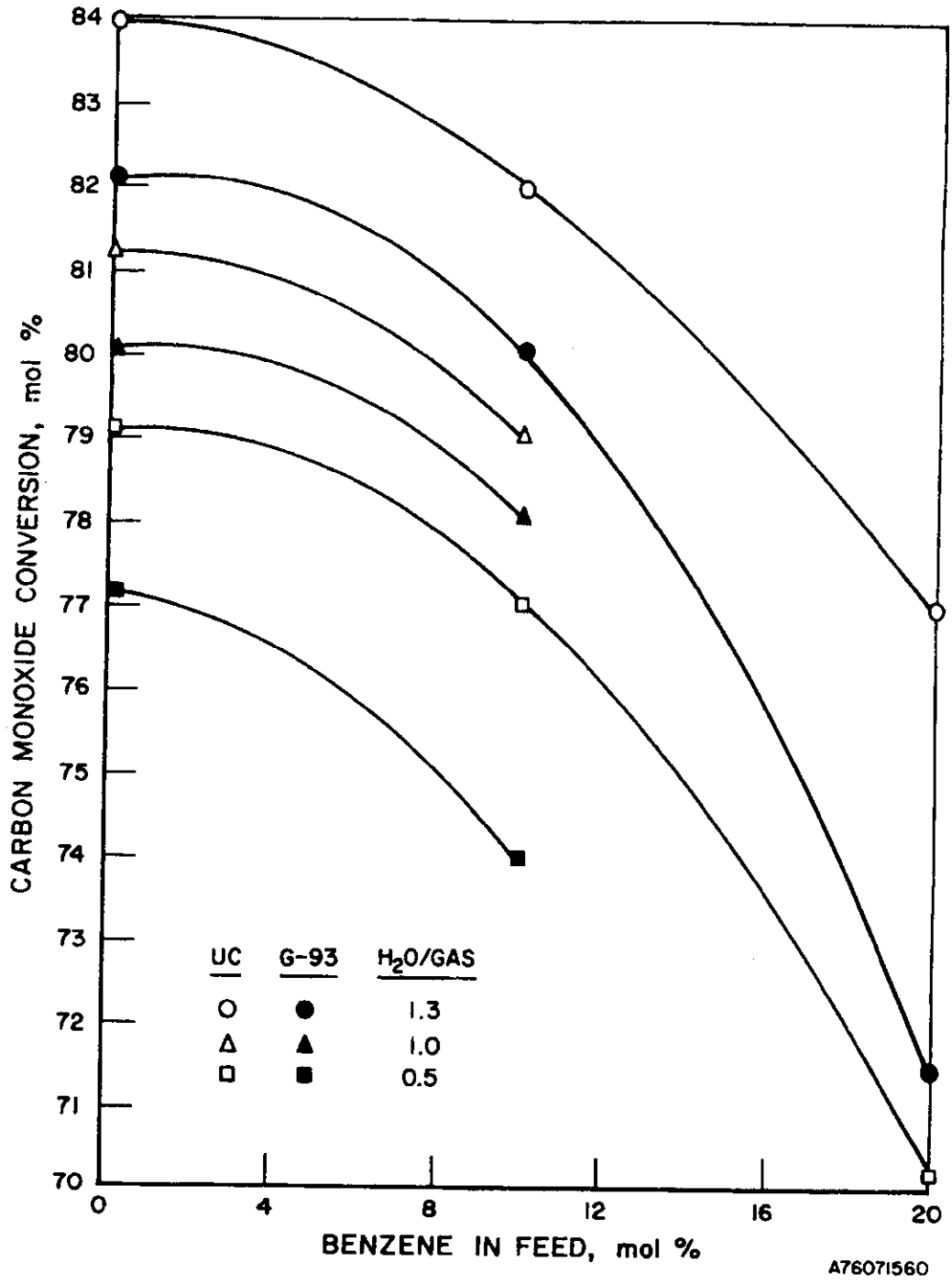

Figure 57. EFFECT OF BENZENE ON CONVERSION OF CARBON MONOXIDE
(At 1000 psig, 650°F, and a CSTR Space Velocity of 0.2300 SCF/hr-g)

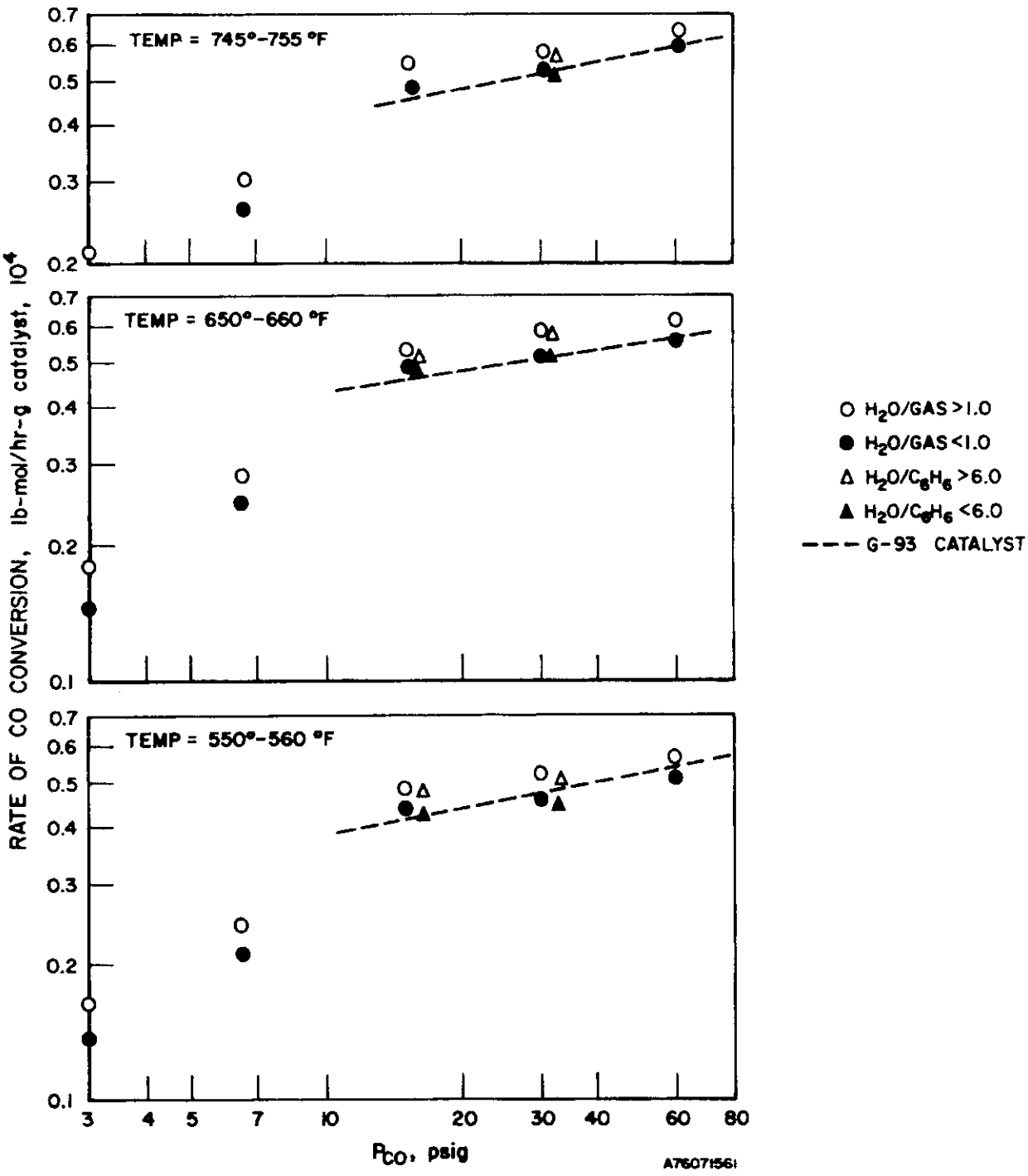

Figure 58. REACTION ORDER OF CARBON MONOXIDE
(UC-1870-46-1 Catalyst, 1/16-in. Extrusions)

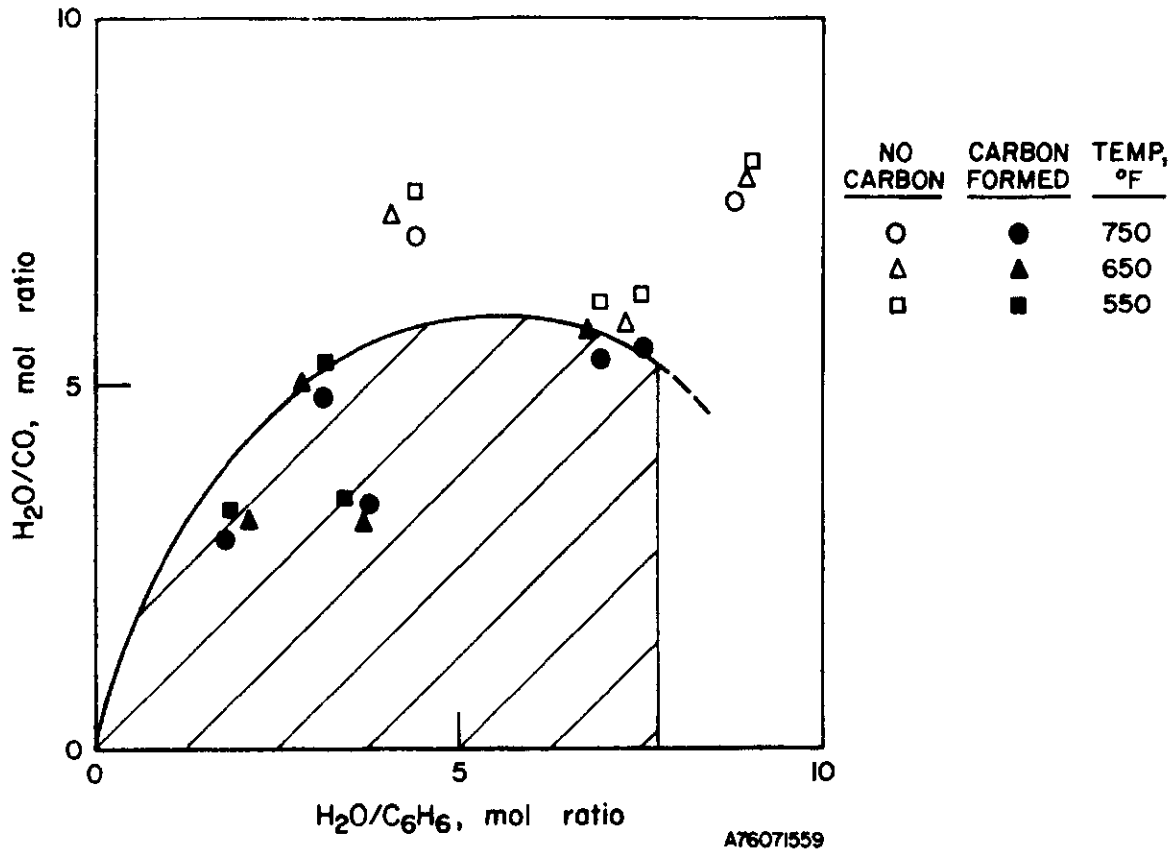

Figure 59. REGIONS OF CARBON FORMATION AS A FUNCTION OF H_2O/CO AND H_2O/C_6H_6 RATIOS
(UC-1870-46-1 Catalyst, 1/16-in. Extrusions)

$$r_o = k_a \bar{C}_m \frac{1/2 p_t/R_g T}{1 + 1/2 K_B p_t/R_g T} = \frac{ap}{1 + bp} \qquad (58)$$

where a and b are the resulting overall constants. This graphically appears as is shown in Figure 60.

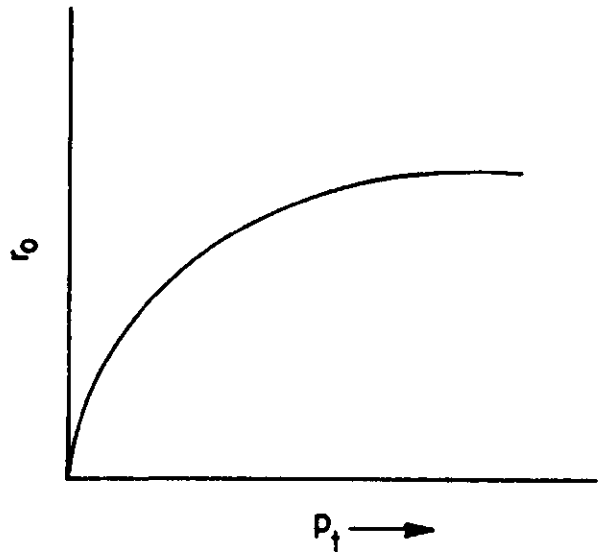

Figure 60. EFFECT OF PRESSURE ON THE INITIAL RATE FOR THE ADSORPTION MECHANISM

For the surface reaction controlling case, Equation 53 becomes —

$$r_o = k_s \bar{C}_m K_A K_B \frac{(1/4) p_t^2/(R_g T)^2}{[1 + (1/2)(K_A + K_B) p_t/R_g T]^2} = \frac{a' p_t^2}{(1 + b' p_t)^2} \qquad (59)$$

and graphically appears as is shown in Figure 61. For the desorption controlling case, Equation 54 becomes —

$$r_o = k_d \bar{C}_m K \frac{(1/4) p_t^2/(R_g T)^2}{1 + (1/2)(K_A + K_B) p_t/R_g T + (1/4) K_C K p_t^2/(R_g T)} \qquad (60)$$

If the equilibrium constant, K, is large with respect to K_a, K_B, and K_C, only the last term in the denominator is important, and the result is —

$$r_o = \frac{k_d \bar{C}_m}{K_C} = a'' \qquad (61)$$

and graphically appears as is shown in Figure 62.

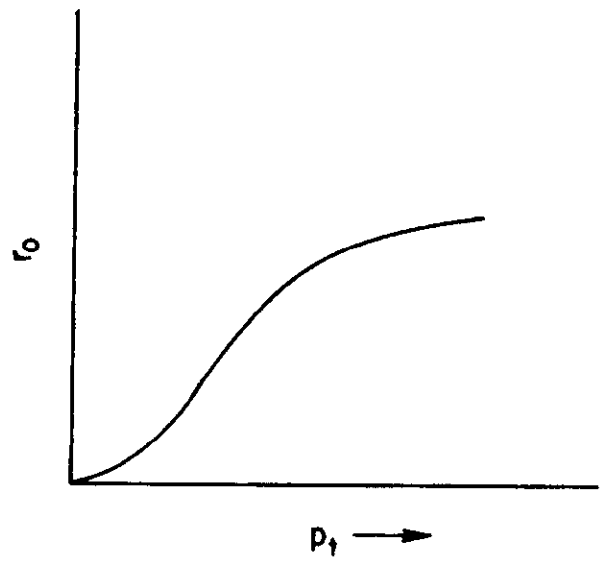

Figure 61. EFFECT OF PRESSURE ON THE INITIAL RATE FOR THE SURFACE REACTION MECHANISM

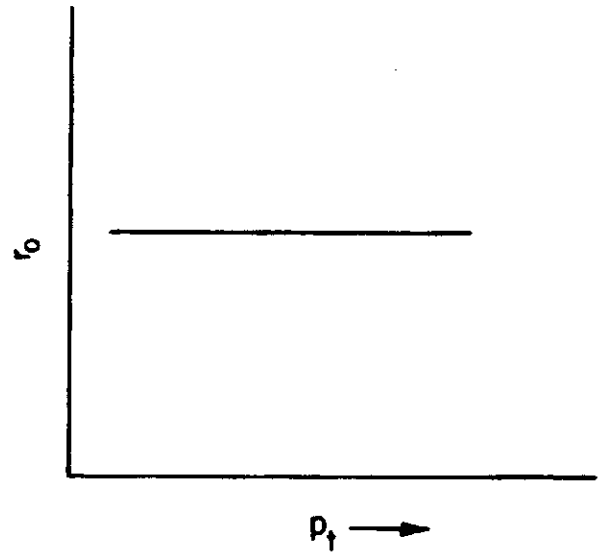

Figure 62. EFFECT OF PRESSURE ON THE INITIAL RATE FOR THE DESORPTION MECHANISM

If the equilibrium constant were not very large for the desorption controlling case, the initial rate equation graph would be the same as that shown in Figure 60.

The experimental rate data were plotted against total pressure, as shown in Figure 63. Based on the above considerations, it appeared that the water-gas shift reaction in our studies was adsorption-desorption controlled. The rate expression developed for the G-93 catalyst, Equation 55, was used to fit these data as a first approximation and is presented in Figure 64. The fit was not satisfactory. A linear regression program was written to fit the data into a form such as that of Equations 53 and 54 with reaction orders of each component as 1.0, and the results are presented in Table 6. The standard deviation, σ, was much too large, which means a poor fit, and, in the case of a better fit (No. 7), the constants were illogical (negative numbers). A better empirical fit, based on the data analysis of each individual component, such as shown in Figures 65 through 68, for all temperatures studied, was obtained with Equation 62.

$$r = \frac{kP_{CO}^{0.5} P_{H_2O}^{0.25}}{1 + C_1P_{CO} + C_2P_{H_2O} + C_3P_{C_6H_6}} \qquad (62)$$

The results are presented in Table 7. An even better fit was obtained for pressures from 0 to 200 psig with the form —

$$r = \frac{kP_{CO}^{0.5} P_{H_2O}^{0.75}}{1 + 0.002P_{H_2O} + 0.01P_{C_6H_6}} \qquad (63)$$

Development of Specific Rate Equations

A number of rate equations have been published, based on iron-chromium or copper-zinc type catalysts rather than cobalt-molybdenum or nickel-molybdenum. These rate equations can be categorized into two distinct forms: the Langmuir-Hinshelwood form and the power-law form. Some of these equations are presented in Table 8 for purposes of illustration. The Langmuir-Hinshelwood form that was used by IGT[5] in its methanation catalysis work was chosen for this study because of the success it enjoyed[6-8]. The experiment design was based on this approach to define the reaction orders with respect to the reactants and products.

The isolation method was used to determine the order of reaction for all the components in the feed. It was found that, for the type of feed compositions studied, the reaction orders of methane, ethane, propane, butane, carbon dioxide, nitrogen, helium, ammonia, and sulfurs are zero. Based on the experimental data obtained using the G-93 catalyst, the following rate equation was developed, as discussed above:

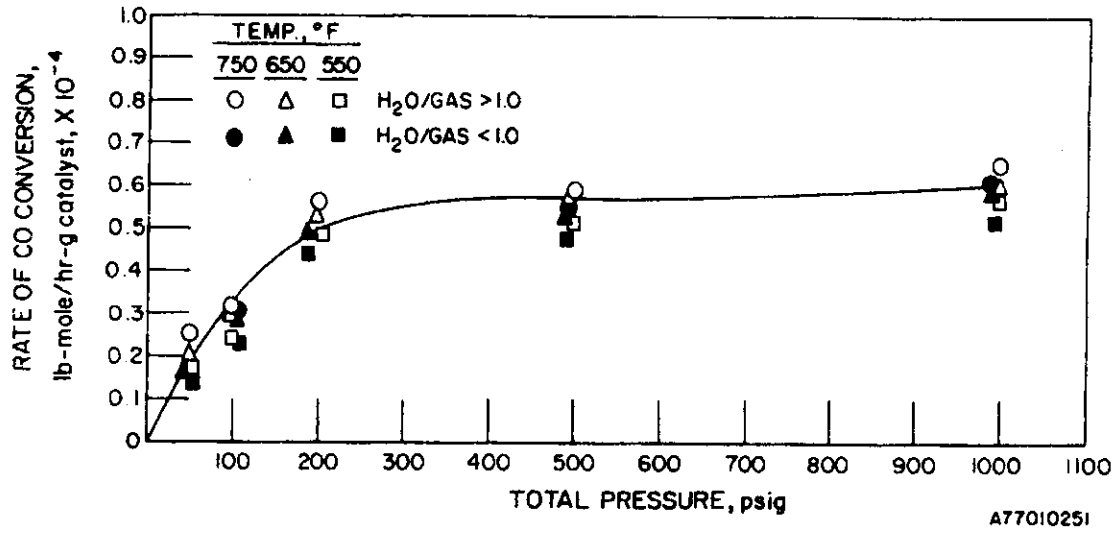

Figure 63. QUALITATIVE ANALYSIS OF RATE EQUATIONS: RATE VERSUS TOTAL PRESSURE FOR THE WATER-GAS SHIFT REACTION (UC-1870-46-1 Catalyst)

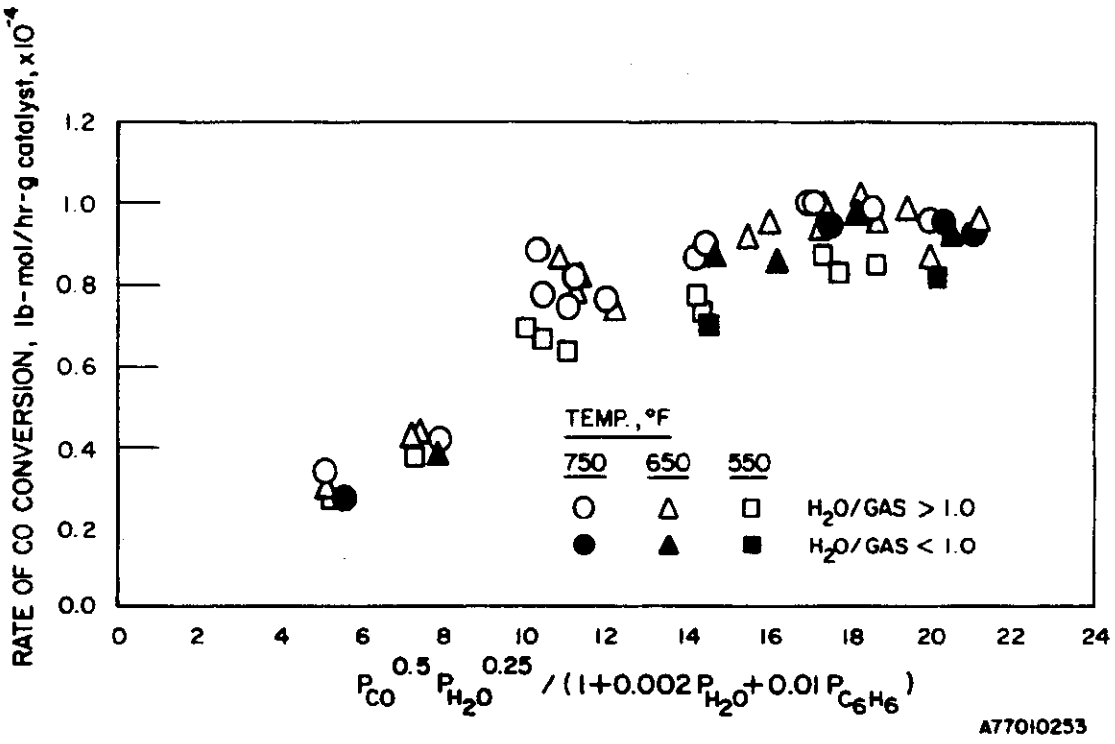

Figure 64. ANALYSIS OF THE RATE EQUATION BASED ON THE DATA USING THE UC-1870-46-1 CATALYST

Table 6. LINEAR REGRESSION ANALYSIS OF DATA (UC-1870-46-1 Catalyst) FOR RATE EQUATION $\sim = kP_{CO}P_{H^2O}/(1 + C_1P_{CO} + C_2P_{H_2O} + C_3P_{C_6H_6})$

Constant	1		2		3		4		5		6		7	
	No.	σ	No.	σ	No.	σ	No.	σ	No.	σ	No.	σ	No.	σ
k	0.02	--	0.1	--	0.1	--	0.1	--	0.1	--	0.019	--	-0.00007	0.000006
C_1	1.613	1.343	0	--	0	--	32.88	3.91	8.47	5.72	1.53	1.28	-0.024	0.0036
C_2	0.185	0.088	9.081	1.82	1.166	0.425	4.49	0.51	0.99	0.47	0.174	0.084	-0.035	0.00045
C_3	0.554	2.235	1.259	0.35	15.80	3.60	-13.99	4.87	2.46	11.2	0.53	2.12	0.003	0.0049

Reproduced from best available copy.

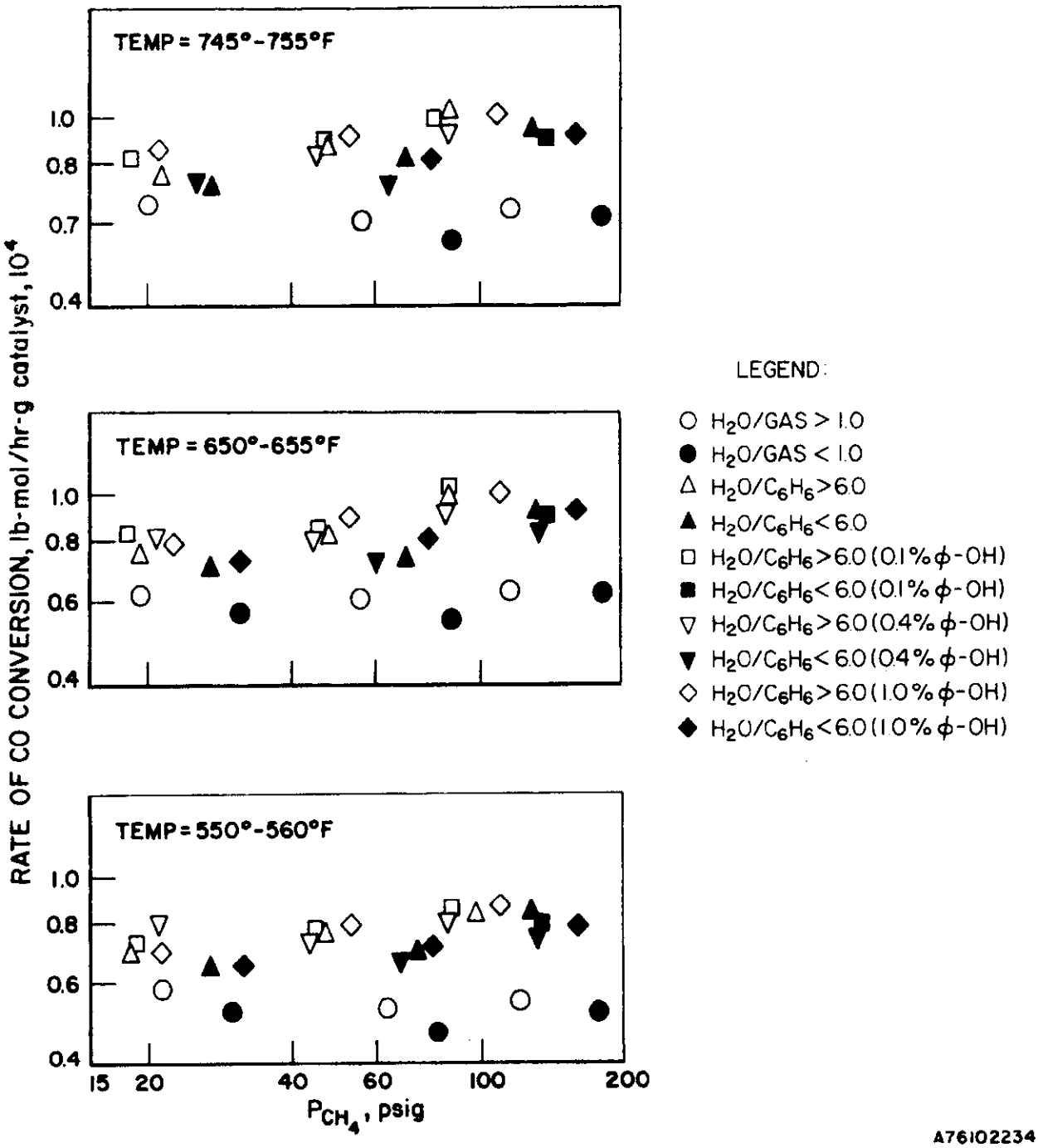

Figure 65. REACTION ORDER OF METHANE (UC-1870-46-1, 1/16-in. Extrusions)

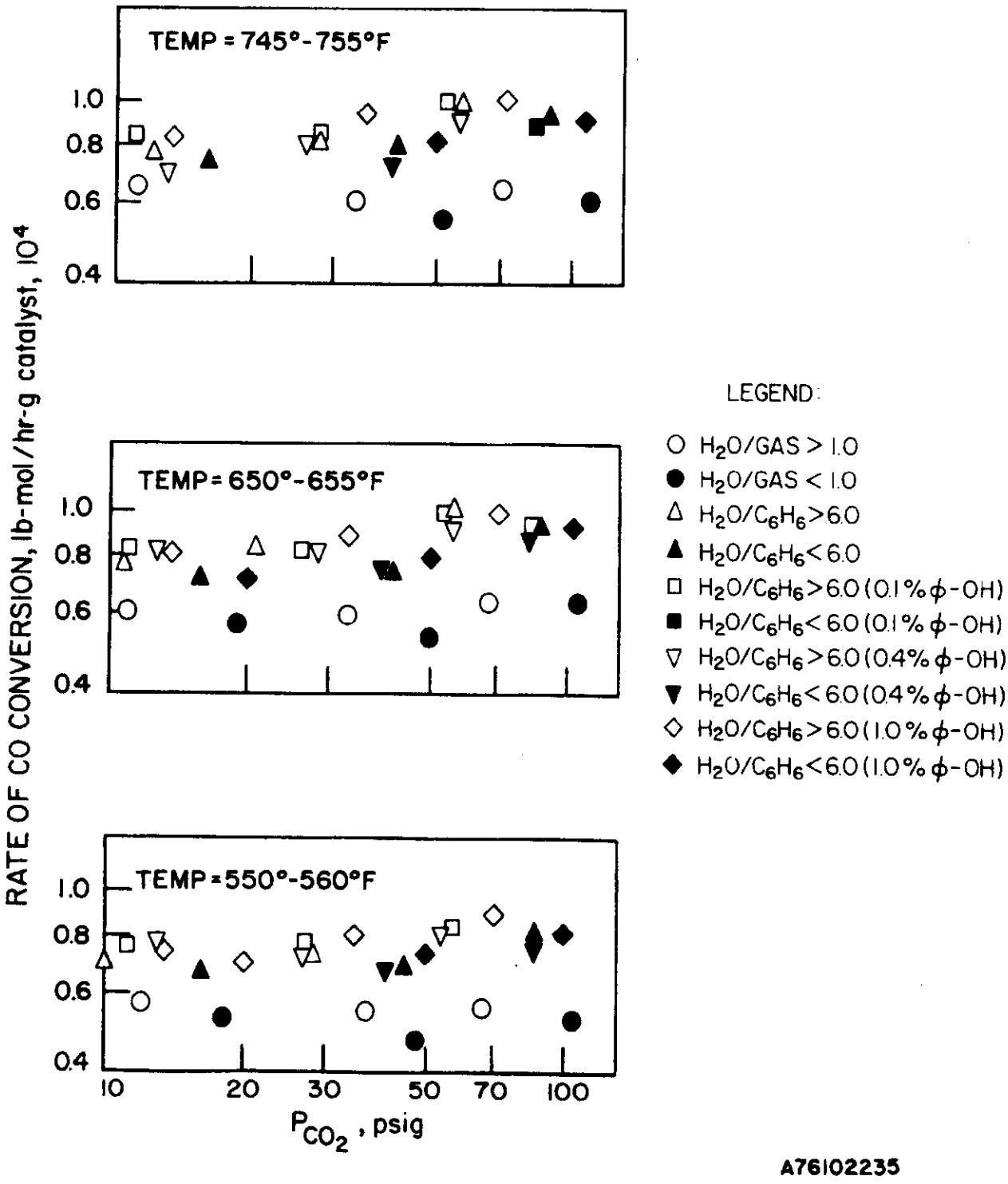

Figure 66. REACTION ORDER OF CARBON DIOXIDE (UC-1870-46-1, 1/16-in. Extrusions)

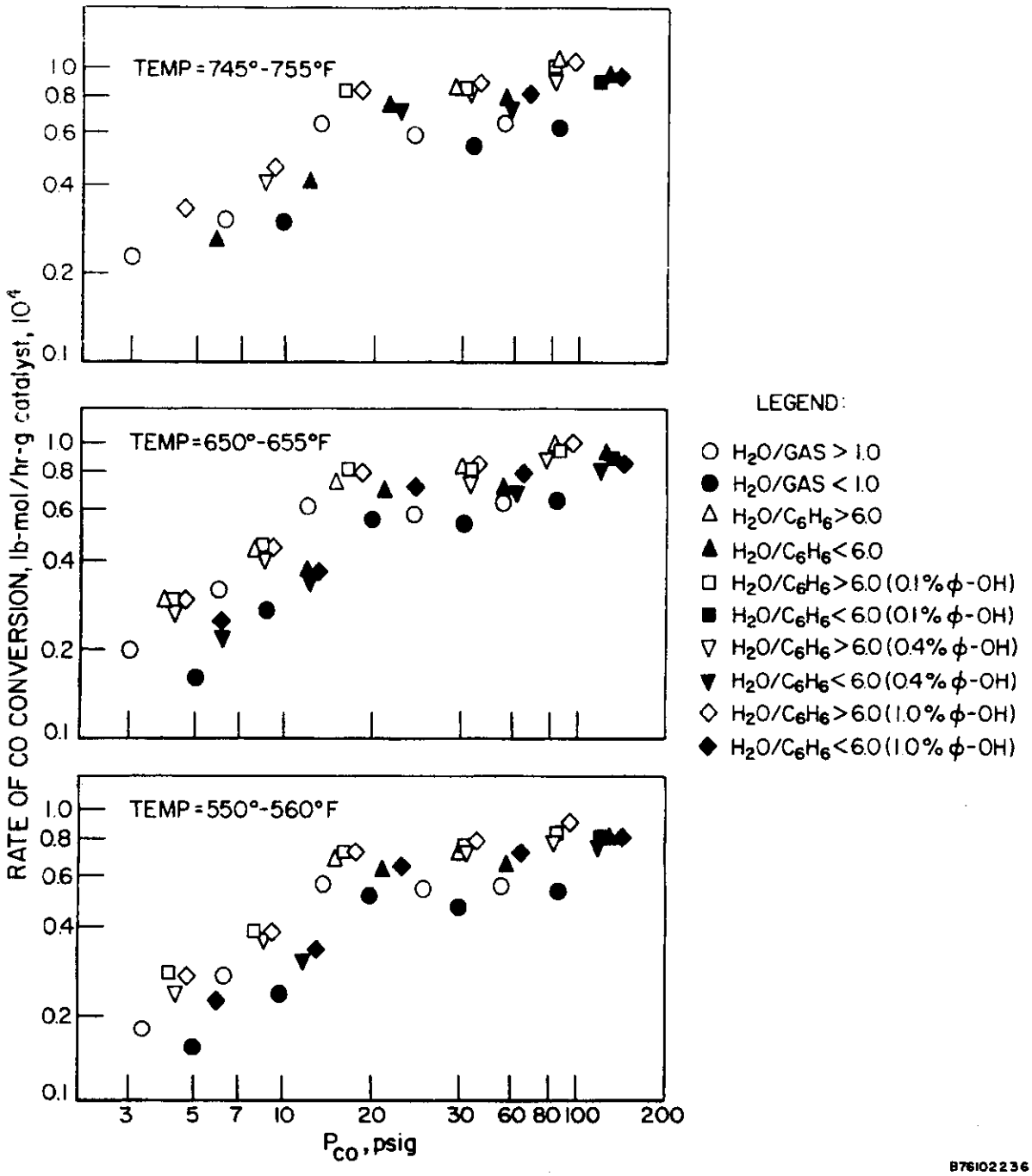

Figure 67. REACTION ORDER OF CARBON MONOXIDE (UC-1870-46-1, 1/16-in. Extrusions)

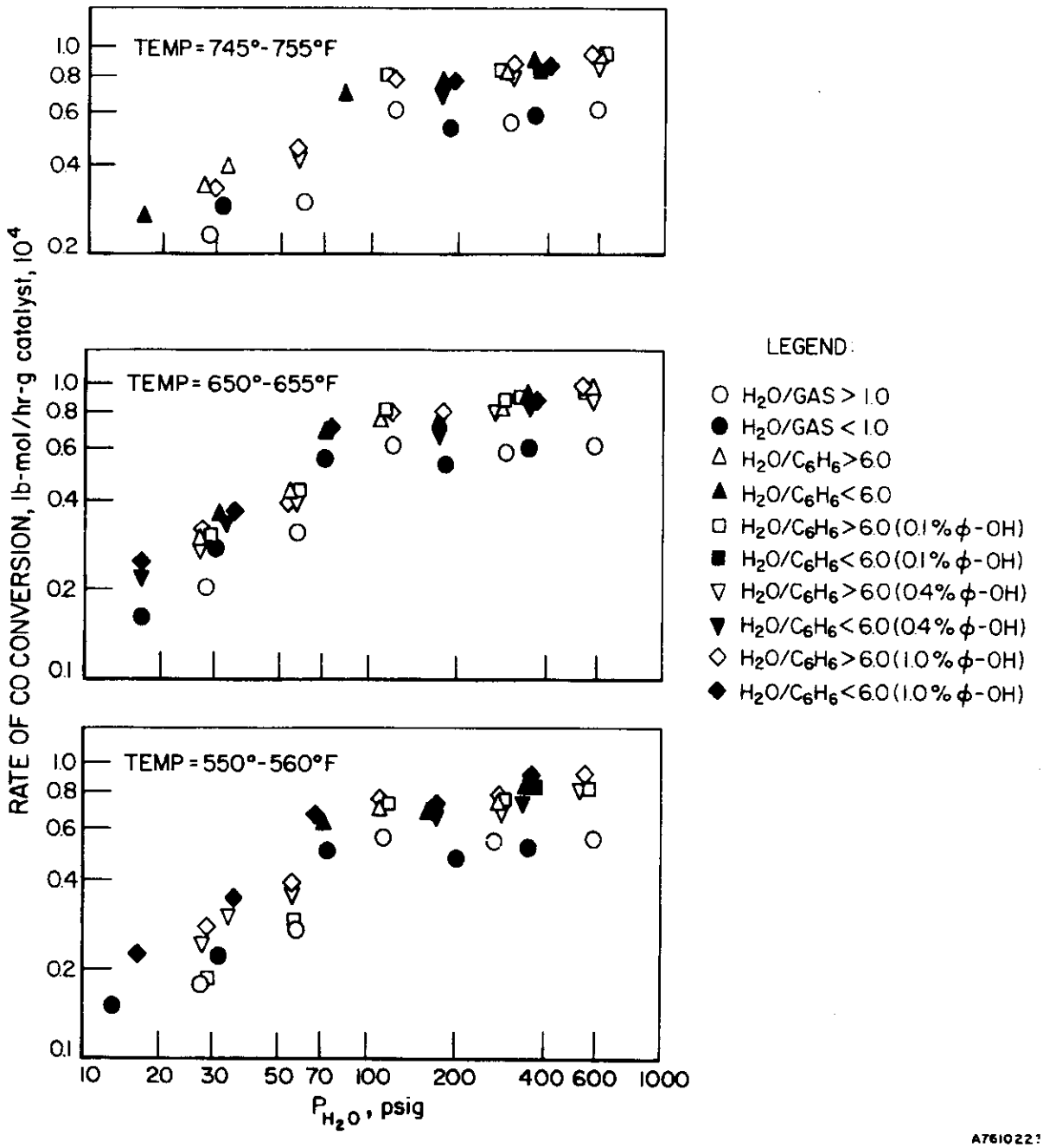

Figure 68. REACTION ORDER OF WATER (UC-1870-46-1, 1/16-in. Extrusions)

Table 7. LINEAR REGRESSION ANALYSIS OF DATA (UC-1870-46-1 Catalyst) FOR RATE EQUATION $r = kP_{CO}^{0.5}P_{H_2O}^{0.25}/(1 + C_1P_{CO} + C_2P_{H_2O} + C_3P_{C_6H_6})$

Constant	1		2		3		4	
	No.	σ	No.	σ	No.	σ	No.	σ
k	0.047	0.0022	0.052	0.0019	--	--	--	--
C_1	0	--	0.014	0.0018	0.345	0.152	0	--
C_2	0.0008	0.0003	0.0005	0.0002	0.051	0.016	0.066	0.015
C_3	0.016	0.002	-0.0002	0.003	0.051	0.239	0.519	0.123

$$r = \frac{kP_{CO}^{0.5}P_{H_2O}^{0.25}}{1 + 0.002\,P_{H_2O} + 0.01\,P_{C_6H_6}} \qquad (64)$$

In anticipation of the low-pressure operation of some of the coal gasification plants or processes, we expanded our pressure studies to include 50 and 100 psig, in addition to 200, 500, and 1000 psig, during the evaluation of the Union Carbide UC-1870-46-1 catalyst. These data were fitted to Equation 64, and a more classical form, such as Equation 65, by a linear regression program. There was no difference in the quality of the fit.

$$r = \frac{kP_{CO}^{0.5}P_{H_2O}^{0.25}}{1 + C_1P_{CO} + C_2P_{H_2O} + C_3P_{C_6H_6}} \qquad (65)$$

A better fit was obtained by changing the reaction orders for the low-pressure range of 0 to 200 psig, and it has the following form:

$$r = \frac{kP_{CO}^{0.5}P_{H_2O}^{0.75}}{1 + 0.002\,P_{H_2O} + 0.01\,P_{C_6H_6}} \qquad (66)$$

To ensure that one of the major reactants, carbon monoxide, has no inhibiting effect on the rate of reaction, carbon monoxide concentration in the feed was increased to 90 mole % (water-free basis), and we found that carbon monoxide does not inhibit the rate of the water-gas shift reaction as long as the steam/gas ratio is higher than 0.5 for the type of multicomponent feeds we used. At steam/gas ratios less than 0.5, carbon formation was detected. To achieve simplicity and to avoid unnecessary terms in a rate equation, Equation 65 type forms are not given further consideration.

Table 8. RATE EQUATIONS FOR WATER-GAS SHIFT REACTIONS PROPOSED BY VARIOUS INVESTIGATORS

Authors	T	P	Catalyst	Rate Equation
Kodama,S.,Mazume,A., Fukuba,K., Fukui,K., "Reaction Rate of Water Gas Shift Reaction." Bull. Chem. Soc. Japan 28 (5), 318-24(1955)	350-400°C	--	Fe_2O_3-Cr_2O_3	$\frac{dP}{dt} = \frac{k_1(P_{CO}P_{H_2O} - K_pP_{CO_2}P_{H_2})}{1 + KP_{CO} + K'P_{H_2O} + K''P_{H_2} + K'''P_{CO_2}}$
Ruthven, D.M., "Note on The Intrinsic Activity of Water Gas Shift Catalysts." Trans. Inst. Chm. Engrs. 46 (6), T185-6 (1968)	350-450°C	--	Fe_2O_3-Cr_2O_3	$r = kP_{CO}P_{H_2O}^{\ell} / P_{CO_2}^{m}$ ℓ, m are a fractional index.
Goodridge,F., Quazi, H.A., "The Water Gas Shift Reaction: A Comparison of Industrial Catalysts."	600-700°K	--	Fe_2O_3-Cr_2O_3 Zn-Cu-Cr	$r = kP_{CO}^{a}P_{H_2O}^{b}P_{CO_2}^{c}P_{H_2}^{d}$ $0.63 < a < 1.41$ $0.53 < b < 0.77$ $-0.3^{1} < c < -0.90$ $-0.31 < d < -0.70$
b. bubp,Khar Kovskii Ploitekhnicheskii Inst. Imeni U.I. Lenena, Kharkov, Trudy 18 (5), 51-60(1958)	400-600°C	atm	Fe_2O_3-Cr_2O_3	$-\frac{dP_{CO}}{dt} = k_1P_{CO}(P_{H_2O}/P_{H_2})^{\beta} - k_2P_{CO_2}(P_{H_2}/P_{H_2O})^{1-\beta}$
Ivanouskii,F.P., Braude,G.E., Semenova,T.A. "A Study of The kinetics of The Reaction of CO and H_2O at High Pressure." Kinetika i Kataliz 5 (3), 563-4(1964)	300-400°C	10,30 atm	Fe_2O_3-Cr_2O_3	$r = k_1P_{CO}(P_{H_2}^{0.5}/P_{H_2}^{0.5}) - k_2P_{CO_2}(P_{H_2}/P_{H_2O})^{0.5}$
Moe,J.M., "Design of Water Gas Shift Reaction" Ch. E. P. 58 (3), 33-36(1962)	600-750°F	--	Fe_2O_3-Cr_2O_3	$r = k(ab - cd/K)$ $\quad a = A - x$ etc.
Bohlbro, H., "The Kinetics of The Water Gas Conversion IV. Influence of Alkali on The Rate Equation." J. Cata. 3, 207-215(1964)	--	--	Fe_2O_3-Cr_2O_3	$r = \frac{k(CO)^{0.75}(H_2O)^{0.30}}{(C)_2)^{0.35}(H_2)^{0.05}}\left(1 - \frac{(CO_2)(H_2)}{K(CO)(H_2O)}\right)$
Lee, A. L., "Evaluation of Shift Catalysts." American Gas Association Project IU-4-9 First Quarter Report, March, 1976	550-750°F	50-1000psig	Co-Mo(G-93)	$r = \frac{kP_{CO}^{0.5}P_{H_2O}^{0.25}}{1 + 0.002P_{H_2O} + 0.01P_{C_6H_6}}$
Lee, A. L., "Evaluation of Shift Catalysts." American Gas Association Project IU-4-9 Annual Report, 1976	550-750°F	0-215 psia	Ni-Mo(UC)	$r = \frac{kP_{CO}^{0.5}P_{H_2O}^{0.75}}{1 + 0.002P_{H_2O} + 0.01P_{C_6H_6}}$

The experimental rate data obatined with all three catalysts (G-93, UC-1870-46-1, and Shell Oil 538) were used separately in the initial analysis of the rate equations. These data were further divided into two pressure ranges, 0 to 200 and 200 to 1000 psig, because of the nature of the rate dependence on pressure. Six specific rate equations with six different rate constants were determined for the water-gas shift reaction using the three different catalysts. They are presented in Table 9, and the total average deviation* from experimental data was about ±10%.

Table 9. SPECIFIC RATE EQUATIONS FOR THE WATER-GAS SHIFT REACTION

$$r = \frac{kP_{CO}^{\ a} P_{H_2O}^{\ b}}{1 + 0.002\ P_{H_2O} + 0.01\ P_{C_6H_6}}$$

Catalyst	50 to 200 psig		200 to 1000 psig	
	a	b	a	b
UC-1870-46-1	0.50	0.75	0.50	0.25
G-93	0.40	0.75	0.50	0.25
Shell Oil 538	0.35	0.75	0.50	0.25

It was found that by keeping the reaction orders constant and by varying the rate constant (which is a function of temperature) only, the same quality of fit can be established. This was a small improvement because it reduced the rate equations from six to one, and the results are presented in Table 10. The rate constants are presented in numerical form rather than as equations to illustrate the sensitivity of the rate dependence on the rate constants.

Table 10. SINGLE RATE EQUATION WITH SPECIFIC RATE CONSTANTS FOR TWO PRESSURE RANGES

$$r = \frac{kP_{CO}^{\ 0.50} P_{H_2O}^{\ 0.25}}{1 + 0.002\ P_{H_2O} + 0.01\ P_{C_6H_6}}$$

Catalyst	50 to 200 psig			200 to 1000 psig		
	k_{750}	k_{650}	k_{550}	k_{750}	k_{650}	k_{550}
UC-1870-46-1	0.084	0.081	0.077	0.063	0.056	0.049
G-93	0.073	0.070	0.063	0.060	0.053	0.047
Shell Oil 538	0.065	0.060	0.056	0.057	0.051	0.046

* Deviation, $\Delta = (r_e - r_{c_n})/r_e$, where r = rate, e = experimental, and c = calculated, $\Delta_{ave} = \sum_1 \Delta_i/n$.

The experimental data were examined carefully, and some were discarded. These data, which are listed in Table 11, were of immature activity, high benzene concentration, or had carbon formation.

Table 11. EXPERIMENTAL DATA NOT USED IN THE RATE ANALYSIS

Catalyst	Run Nos.
UC-1870-46-1	1 to 12, 29 to 31
G-93	1 to 4, 44 to 49, 99, 102 to 104, 106 to 109
Shell Oil 538	1 to 6, 12 to 14, 72 to 74, 81 to 83, 90 to 92, 108

The remainder of the data were used in the development of a generalized rate equation. These data were plotted for each catalyst used and are presented in Figures 69 through 72. The rate equations were further simplified by reducing the rate constants from six to three. These rate constants in Arrhenius form and the average deviations are presented in Table 12. Based on these rate constants, the calculated rates of reaction are compared with the experimental values and are presented in Appendix C, Tables C-1 through C-3.

Study of Surface-Reaction-Controlled Rates

The rates analyses completed so far were based on the assumptions that the reaction rates were adsorption/desorption controlled. The fit of the proposed rate equations to the experimental values is considered to be good in heterogeneous catalytic kinetics. However, the acute pressure dependence of the rates on pressures at 200 psig and less requires closer attention. To ensure that the rate-controlling step has not changed drastically from adsorption/desorption to surface reaction or vice versa, the experimental data were fitted in a surface-reaction-controlled rate equation, which has the form of Equation 67, and the results are presented in Appendix C, Tables C-4 through C-6.

$$r = \frac{k P_{CO}^{0.5} P_{H_2O}^{0.25}}{(1 + 0.002\, P_{H_2O} + 0.01\, P_{C_6H_6})^2} \qquad (67)$$

The rate constants and the average deviations are presented in Table 13, and the fit is presented in Figure 73.

To ensure that the rate-controlling step is not somewhere between adsorption-surface reaction-desorption, calculated values from Equation 68

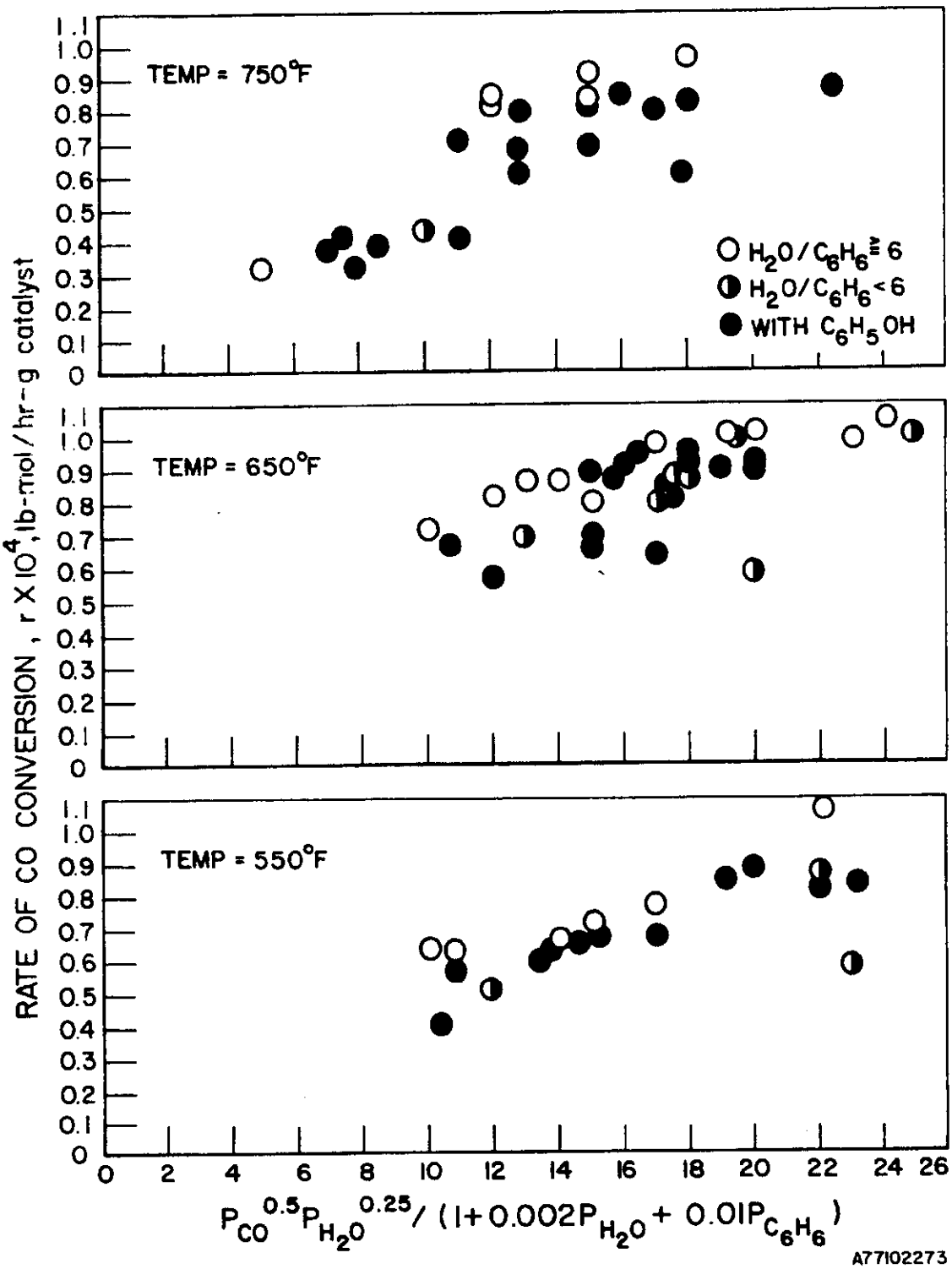

Figure 69. DETERMINATION OF THE RATE CONSTANT FOR THE WATER-GAS SHIFT REACTION (G-93 Catalyst)

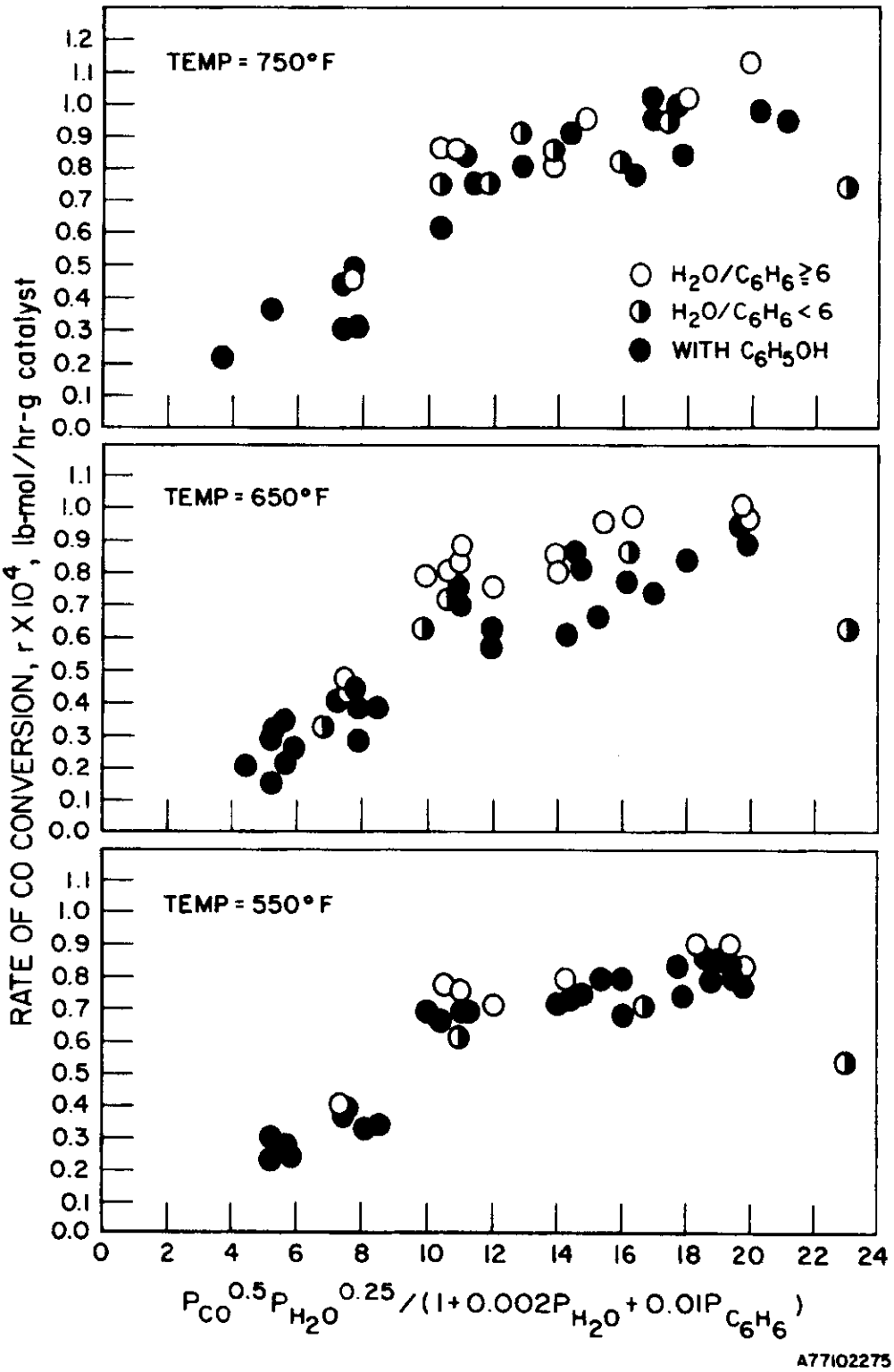

Figure 70. DETERMINATION OF THE RATE CONSTANT FOR THE WATER-GAS SHIFT REACTION (UC-1870-46-1 Catalyst)

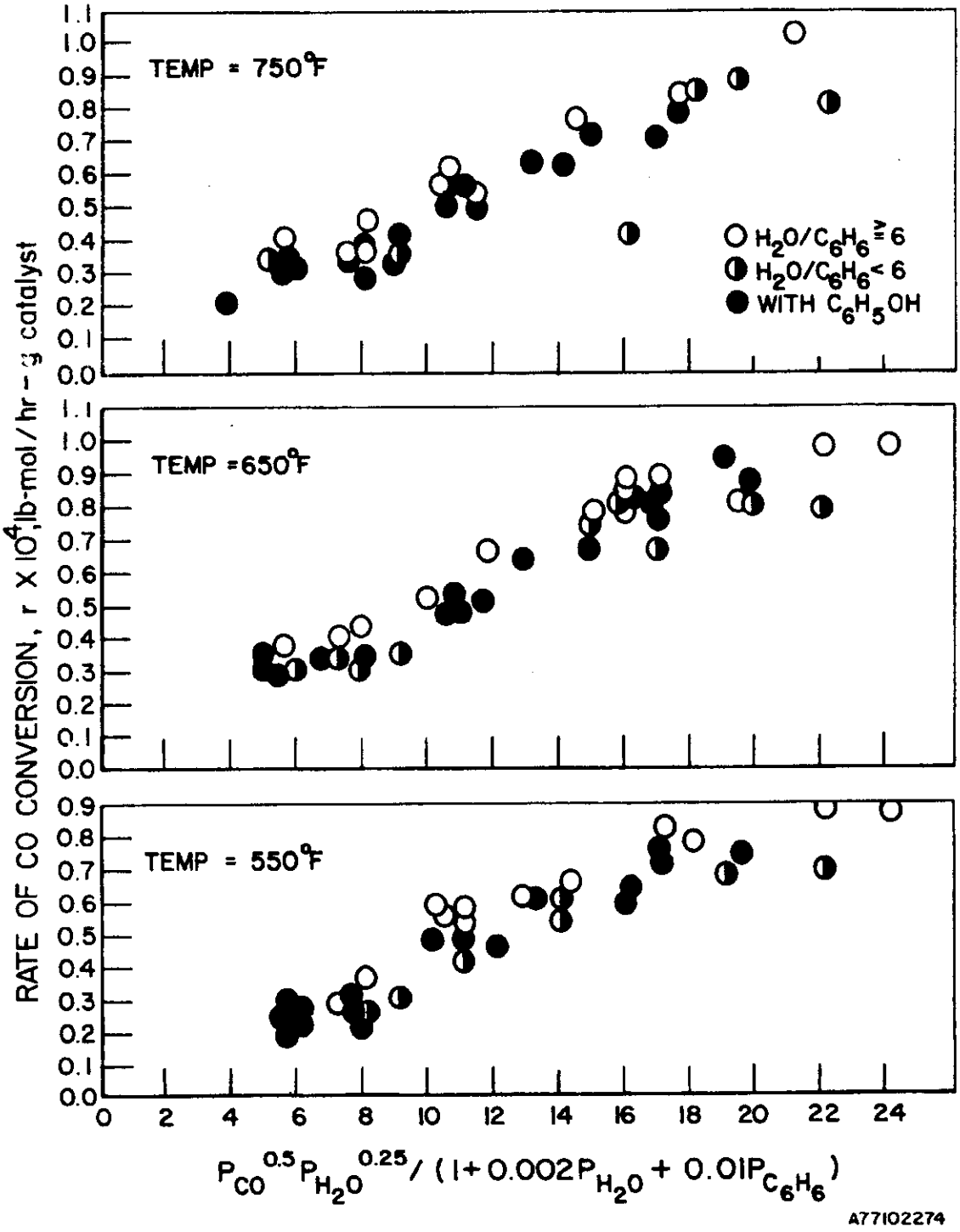

Figure 71. DETERMINATION OF THE RATE CONSTANT FOR THE WATER-GAS SHIFT REACTION (Shell Oil 538 Catalyst)

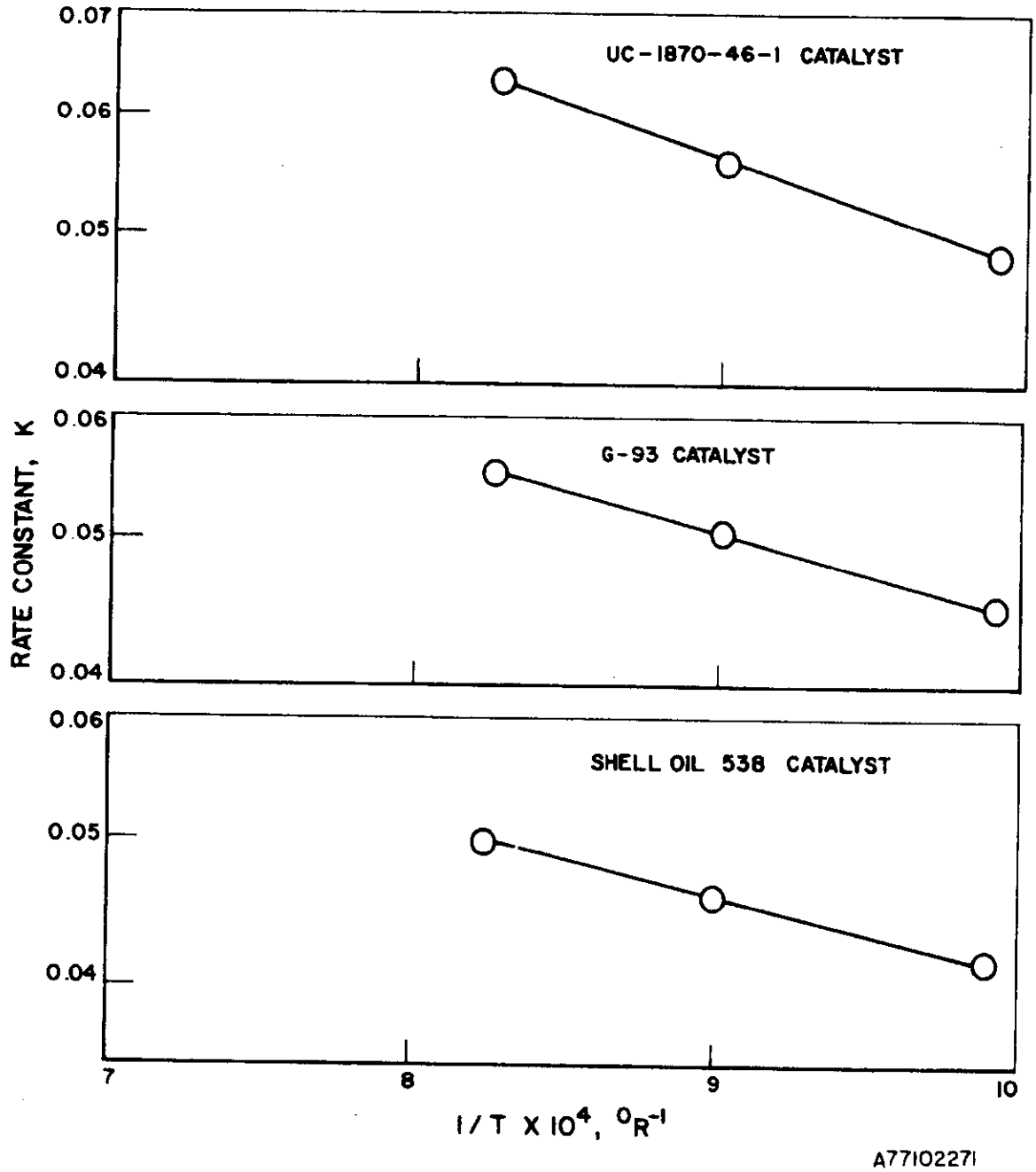

Figure 72. ARRHENIUS PLOT FOR THE WATER-GAS SHIFT REACTION BASED ON THE RATE EQUATIONS DEVELOPED FOR EACH CATALYST

Table 12. SINGLE RATE EQUATION WITH SPECIFIC RATE CONSTANTS FOR ALL PRESSURES

Catalyst	Rate Constant, k	Average Deviation, % 550°F	650°F	750°F
UC-1870-46-1	0.23exp (-3120/RT)	±13	±11	±11
G-93	0.16exp (-2530/RT)	±11	±10	±8
Shell Oil 538	0.11exp (-1950/RT)	±7	±9	±9

Table 13. RATE CONSTANTS AND DEVIATIONS FOR A SURFACE-CONTROLLED RATE EQUATION

Catalyst	Rate Constant	Average Deviation, % 550°F	650°F	750°F
UC-1870-46-1	0.39exp (-2930/RT)	±38	±38	±32
G-93	0.33exp (-3000/RT)	±39	±28	±27
Shell Oil 538	0.36exp (-3940/RT)	±30	±28	±30

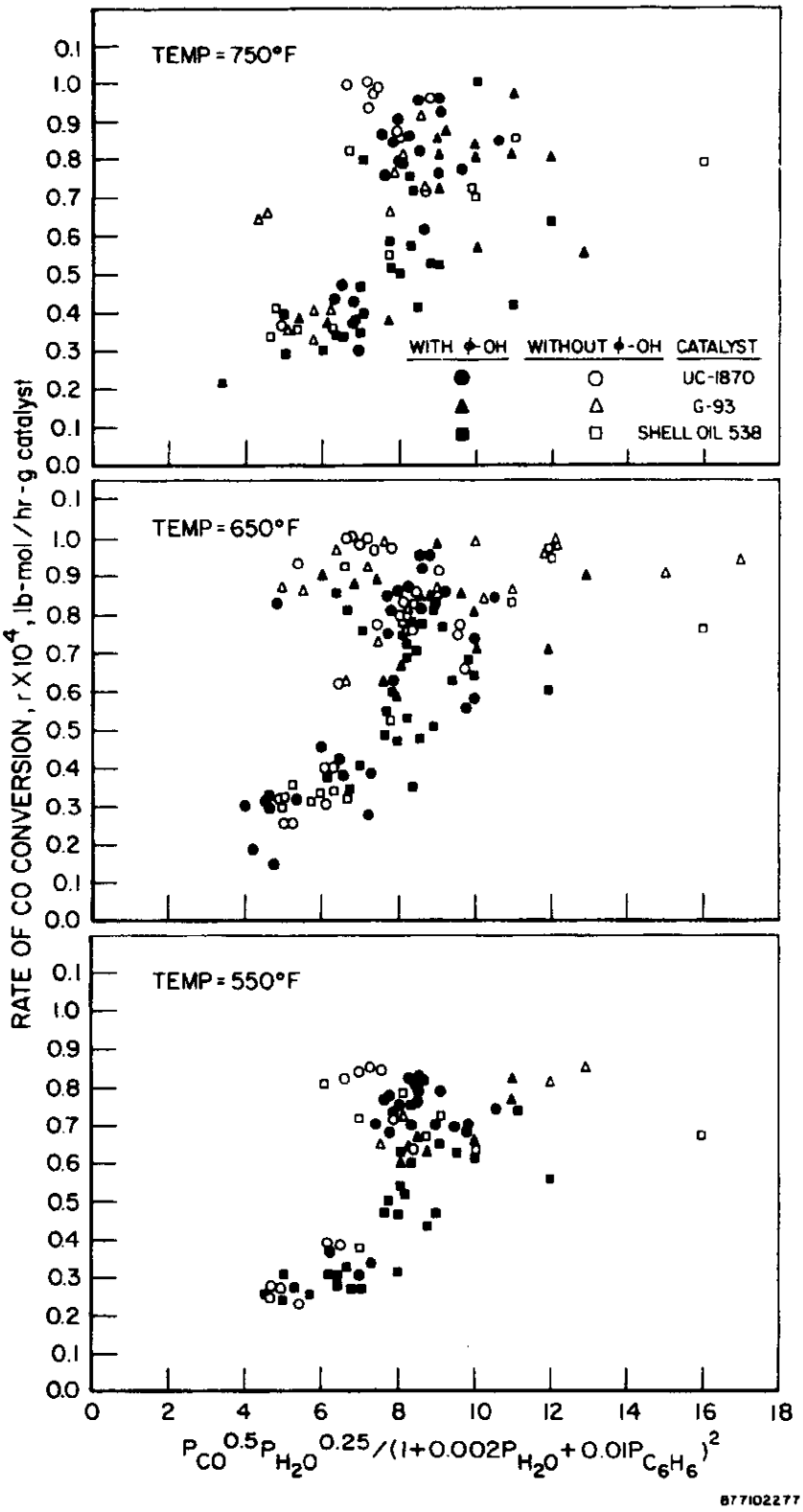

Figure 73. ANALYSIS OF RATE DATA -- DETERMINATION OF A GENERALIZED RATE EQUATION BASED ON SURFACE REACTION CONTROL RATE

were compared with experimental data, and the results are also presented in Tables C-4 through C-6 and in Figure 74. The rate constants and the average deviations are presented in Table 14.

Table 14. RATE CONSTANTS AND DEVIATIONS FOR A SURFACE-REACTION/ADSORPTION/DESORPTION CONTROLLED RATE EQUATION

Catalyst	Rate Constant	Average Deviation, % 550°F	650°F	750°F
UC-1870-46-1	0.19exp (-1960/RT)	±25	±28	±25
G-93	0.19exp (-2250/RT)	±28	±22	±22
Shell Oil 538	0.16exp (-2100/RT)	±22	±23	±25

$$r = \frac{k P_{CO}^{0.5} P_{H_2O}^{0.25}}{(1 + 0.002\ P_{H_2O} + 0.01\ P_{C_6H_6})^{1.5}} \qquad (68)$$

As can be seen from Figure 70 through 74, the best fit obtained was based on the adsorption/desorption model.

Development of General Rate Equation

Based on the form of Equation 64 and the average value from Table 12, a generalized rate equation for the water-gas shift reaction using all three catalysts was developed. It has the following form:

$$r = \frac{0.17\ \exp\ (-E/RT) P_{CO}^{0.5} P_{H_2O}^{0.25}}{1 + 0.002\ P_{H_2O} + 0.01\ P_{C_6H_6}} \qquad (69)$$

where —

r = rate, 10^{-4} lb-mol/hr-g catalyst

P = partial pressure, psia

E = activation energy, 2650 Btu/lb-mol

T = temperature, °R

R = gas constant, 1.986 Btu/lb-mol/°R.

The calculated vales and deviations of each data point are listed in Tables C-1 through C-3. The experimental values and the calculated values based upon the specific rate constants are also listed in these tables for comparison purposes. The average deviations are summarized in Table 15. The fit by the generalized equation is acceptable and is presented in

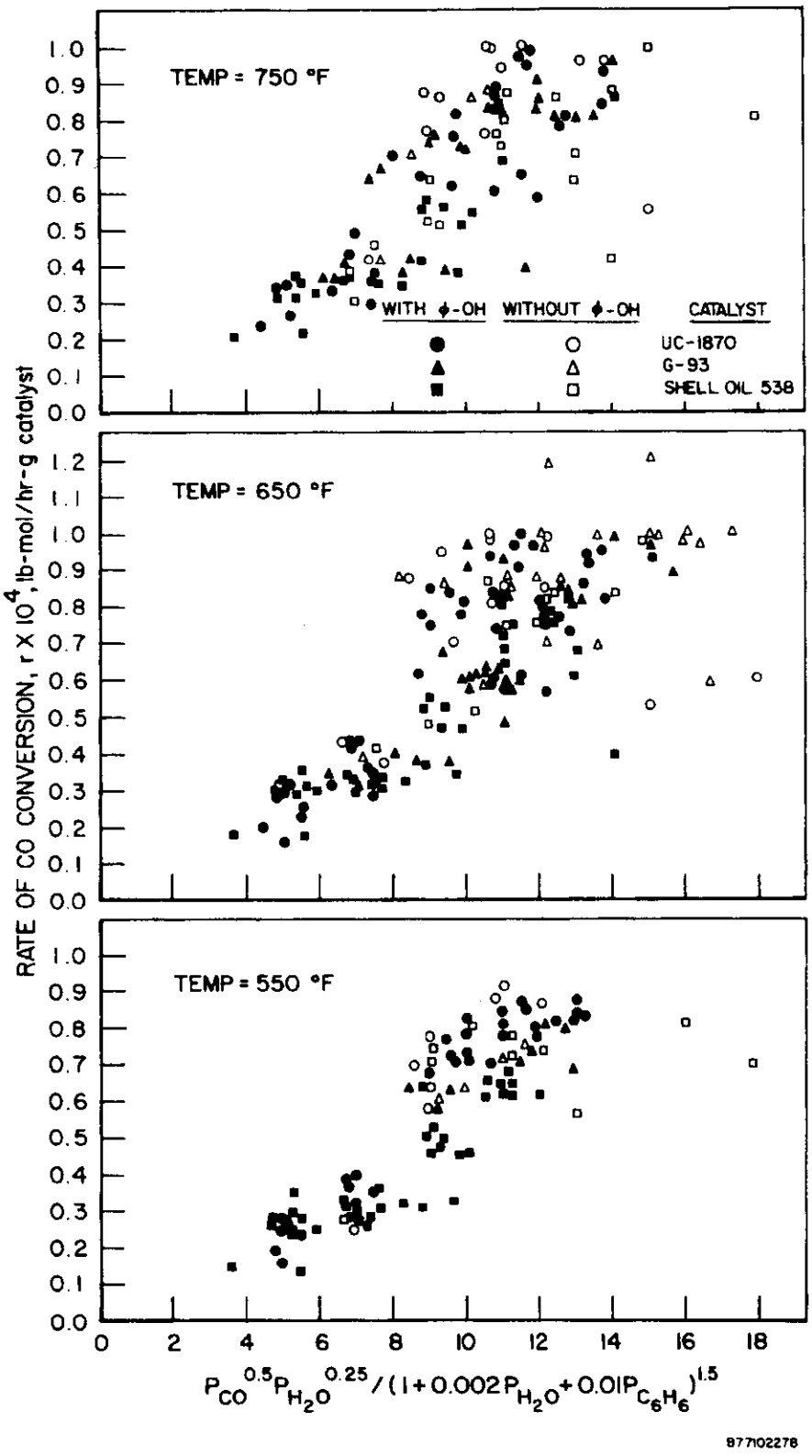

Figure 74. ANALYSIS OF RATE DATA — DETERMINATION OF A GENERALIZED RATE EQUATION BASED ON ADSORPTION/SURFACE REACTION CONTROL RATE

Figures 75 and 76. The generalized equation fits the data for all three catalysts without excessive sacrifice in the accuracy of prediction.

Table 15. AVERAGE DEVIATION OF THE GENERALIZED RATE EQUATION FROM EXPERIMENTAL DATA

Catalyst	550°F	650°F	750°F
UC-1870-46-1	±13	±12	±14
G-93	±11	±12	±9
Shell Oil 538	±13	±10	±14

Analysis of Carbon Formation

The experimental work showed that the presence of a large amount of benzene in the feed promotes carbon formation, and steam inhibits it. The amount and rate of carbon formation were proportional to the amount of benzene in the feed and were inversely proportional to the amount of steam in the feed.

In their partial oxidation processes and their work prior to submitting the catalysts for evaluation, BASF used a steam/gas ratio of 1.2. Shell Oil used a ratio of 1.0 to 1.5, and Union Carbide a ratio of 1.2. Girdler Chemical used a ratio of 0.8 to 1.5, depending upon the concentration of carbon monoxide in the feed. In the presence of 10 mole % benzene, Girdler Chemical experienced no carbon formation at a water/gas ratio of 1.0; Union Carbide experienced no carbon formation at a water/gas ratio of 1.2; and Shell Oil experienced some carbon formation at a water/gas ratio of 1.0.

Figure 77 shows the feed gas composition range which led to carbon formation in tests with the G-93 catalysts.

Although, at the temperatures that we studied, equilibrium favors carbon deposition by $2\ CO \rightleftarrows CO_2 + C$, the reaction rate is often too slow for carbon to develop. For this reason, many commercial methanators for hydrogen and ammonia production are able to operate at conditions where carbon formation is favored but does not occur.

The possible carbon formation reactions in our system were listed earlier as Reactions 38 through 44. Reaction 44 may be neglected in this analysis because we have not experienced a methane loss. Generally, it is assumed that Reactions 41 and 42 do not take place as written, but occur as follows:

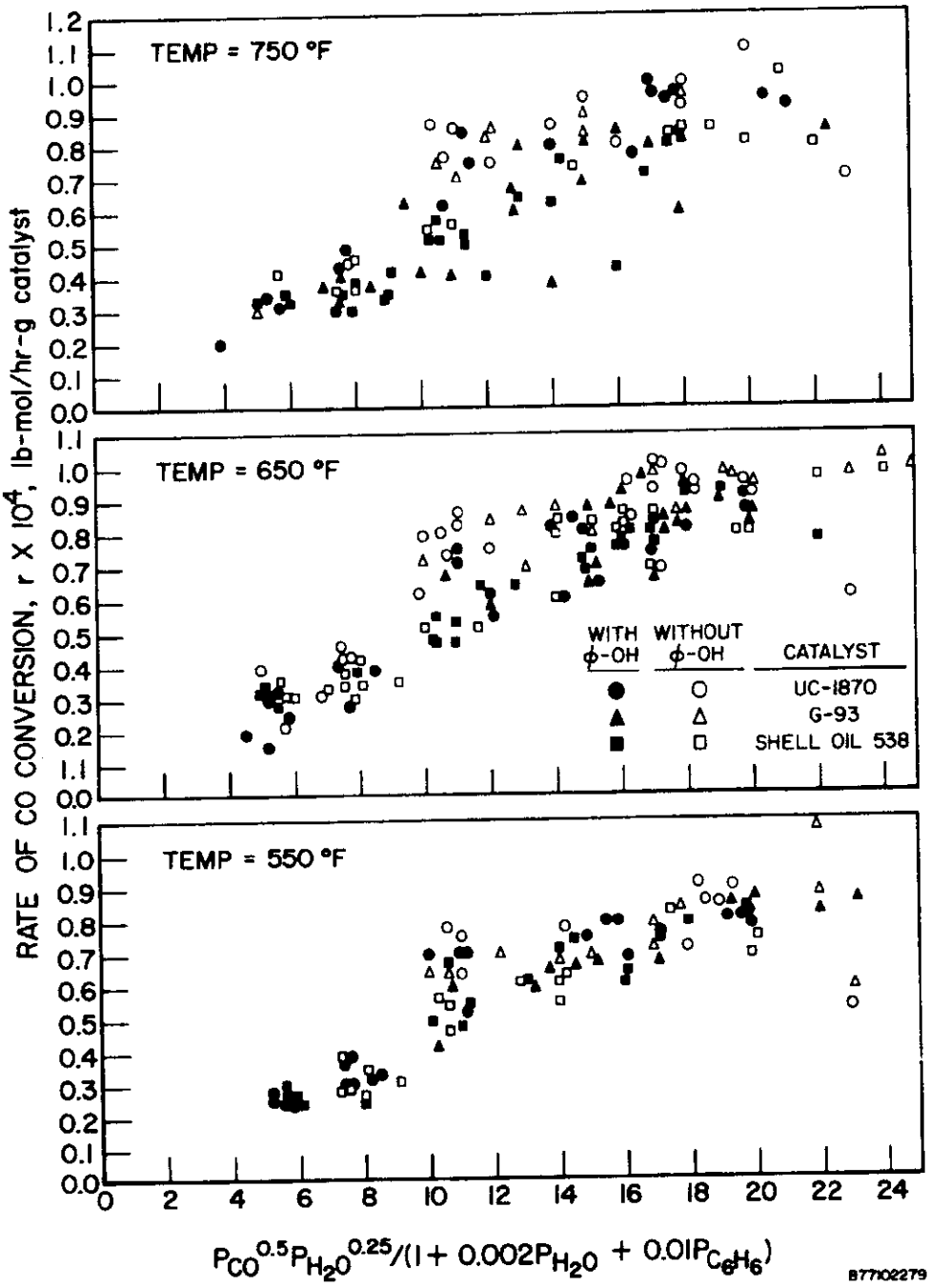

Figure 75. ANALYSIS OF RATE DATA — DETERMINATION OF A GENERALIZED RATE EQUATION BASED ON ADSORPTION/DESORPTION CONTROL RATE

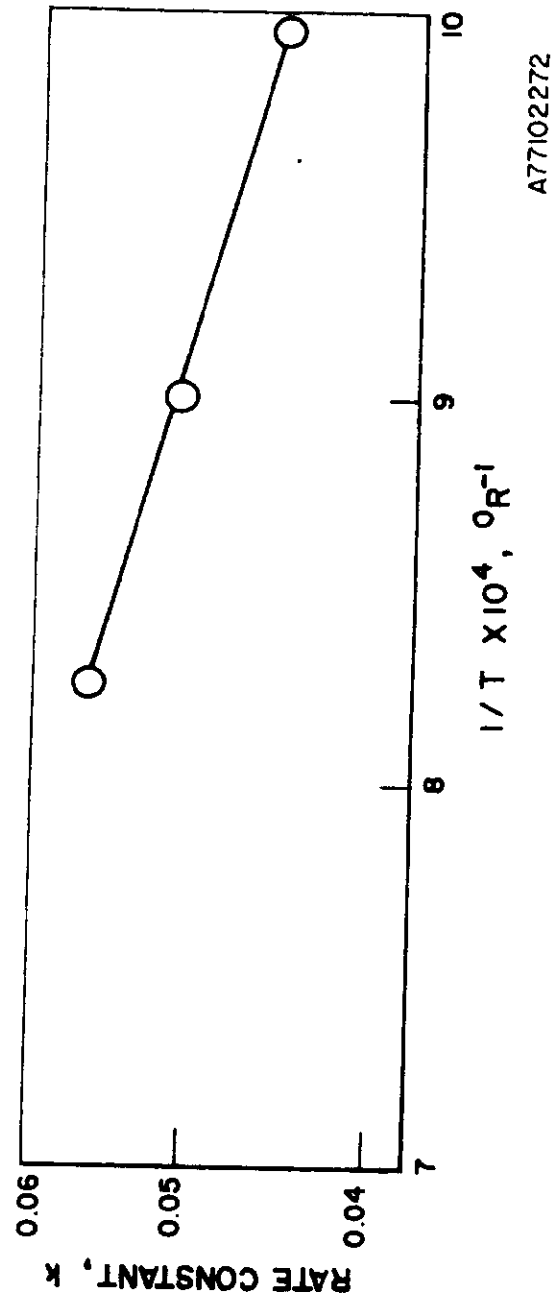

Figure 76. ARRHENIUS PLOT FOR THE WATER-GAS SHIFT REACTION BASED ON THE GENERALIZED RATE EQUATION, $r = kP_{CO}^{0.5} P_{H_2O}^{0.25}/(1 + 0.002 P_{H_2O} + 0.01 P_{C_6H_6})$

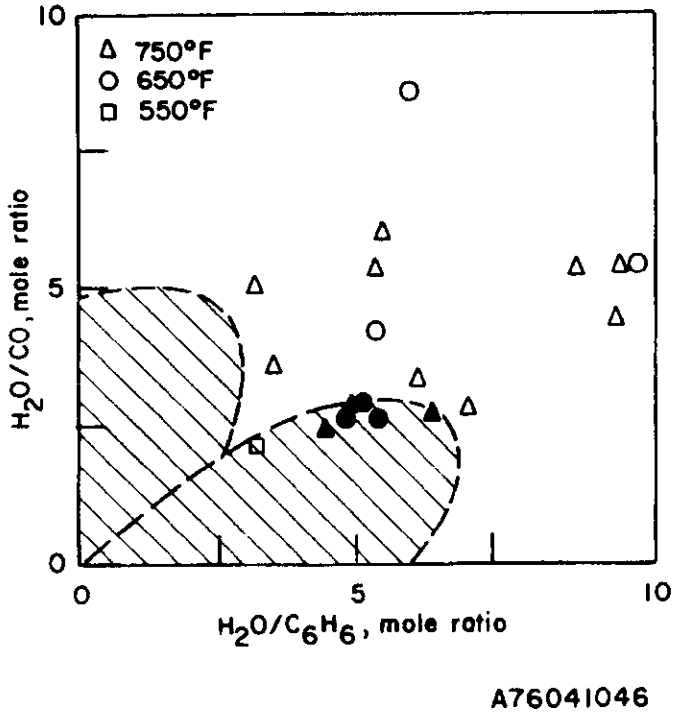

Figure 77. REGIONS OF CARBON FORMATION AS A FUNCTION OF H_2O/CO AND H_2O/C_6H_6 MOLE RATIOS (G-93 Catalyst)

$$\begin{array}{rl} 2CO & \rightleftarrows CO_2 + C \\ + CO_2 + H_2 & \rightleftarrows H_2O + CO \\ \hline CO + H_2 & \rightleftarrows H_2O + C \end{array} \qquad (70)$$

and

$$\begin{array}{rl} 2CO & \rightleftarrows CO_2 + C \\ + 2CO_2 + 2H_2 & \rightleftarrows 2H_2 + 2CO \\ \hline CO_2 + 2H_2 & \rightleftarrows 2H_2O + C \end{array} \qquad (71)$$

A catalyst that promotes the water-gas shift reaction also promotes the reverse of Reactions 70 and 71. Carbon is not formed unless the steam concentration becomes low.

It is possible for Reaction 43 to occur in the presence of iron, steel, and sulfides, which are catalysts for carbon deposition, particularly in laboratory-scale reactors where the surface/volume ratio is relatively large. It is also possible that, at low steam/gas ratios, benzene interferes with the reverse of Reactions 70 and 71 by blocking the water from the active sites and promoting carbon formation.

Many papers dealing with carbon formation can be found in the literature, including an early, well-known one by Dent et al.[1] They postulated that the mechanism of methanation and water-gas shift reactions involves the formation of chemisorbed carbon atoms, which are then reacted to methane or carbon dioxide. If the reaction rates are fast enough to avoid the linkage of chemisorbed carbon atoms, there will be no carbon deposition.

More recent works dealing with the prediction of carbon formation are those of White et al.[3] and Gruber.[2] The work of White et al. led to two graphs, which are reproduced as Figures 78 and 79. They show carbon formation equilibrium isotherms as weight fractions on a triangular diagram, based on Reactions 38 through 44. The area above the isotherm favors carbon formation, and that below does not. The effect of temperature on carbon formation is presented in Figure 78, and the effect of pressure is presented in Figure 79. It can be seen that the steam/gas ratio is important not only in the rate of the water-gas shift reaction, but also in carbon formation.

Analysis of the Reversible Poisoning by Ammonia

The presence of ammonia deactivated the catalyst when the sulfur concentration in the feed became low. The activity of the catalyst gradually returned to normal if the sulfur content in the feed was increased and the flow of ammonia was stopped. This poisoning effect can be avoided by either thoroughly pretreating the fresh catalyst with hydrogen sulfide, carbon disulfide, or carbonyl sulfide prior to the water-gas shift reaction, or, for the newer catalysts, by maintaining the sulfur concentration in the feed above one mole percent (dry basis).

This reversible poisoning effect may be explained by the theory that a) the poisons are chemisorbed on preadsorbed reactants on the catalyst, and b) the activity of the catalyst is strongly dependent upon the method of preparation. The catalyst possesses a number of active sites, A, and to account for the observed change in rate with time that occurs following any change in the reactants partial pressures, we propose that the active sites do not enter into the reaction directly. Instead, the reaction takes place at an effective site, ES, which is produced in this case by sulfiding. If we let X = the poisoned sites, the following reactions may be written:

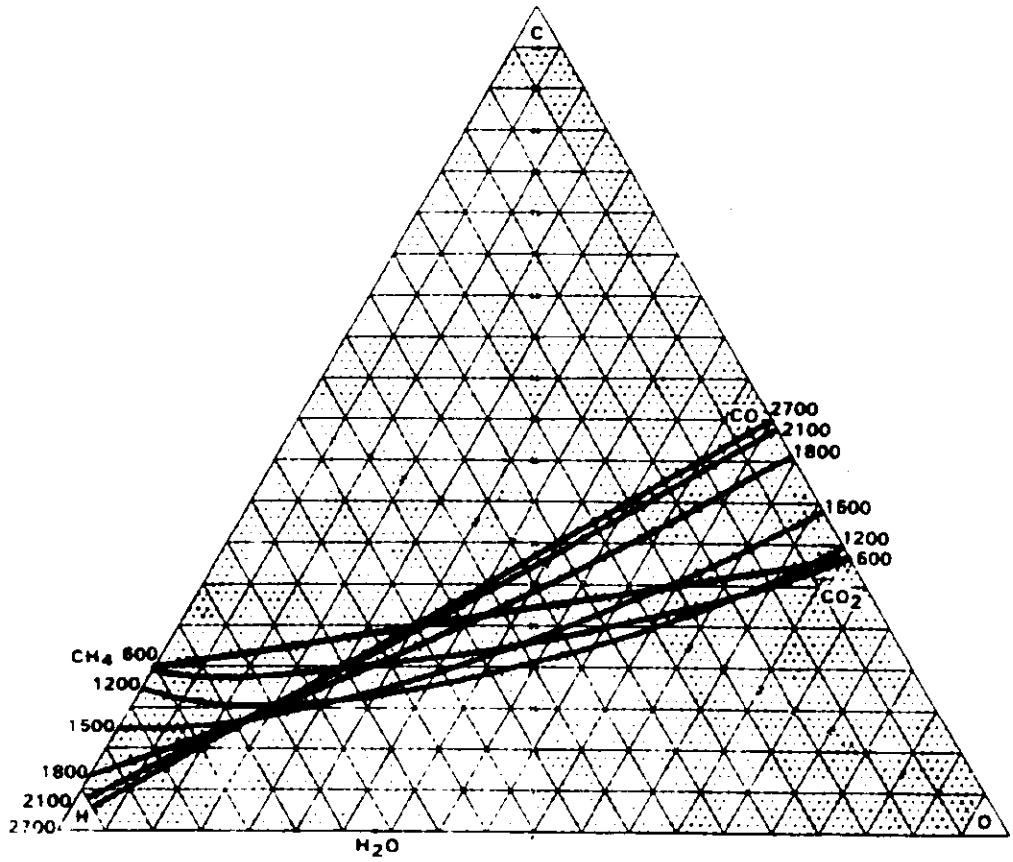

Figure 78. CARBON FORMATION EQUILIBRIUM ISOTHERMS AT 400 psia

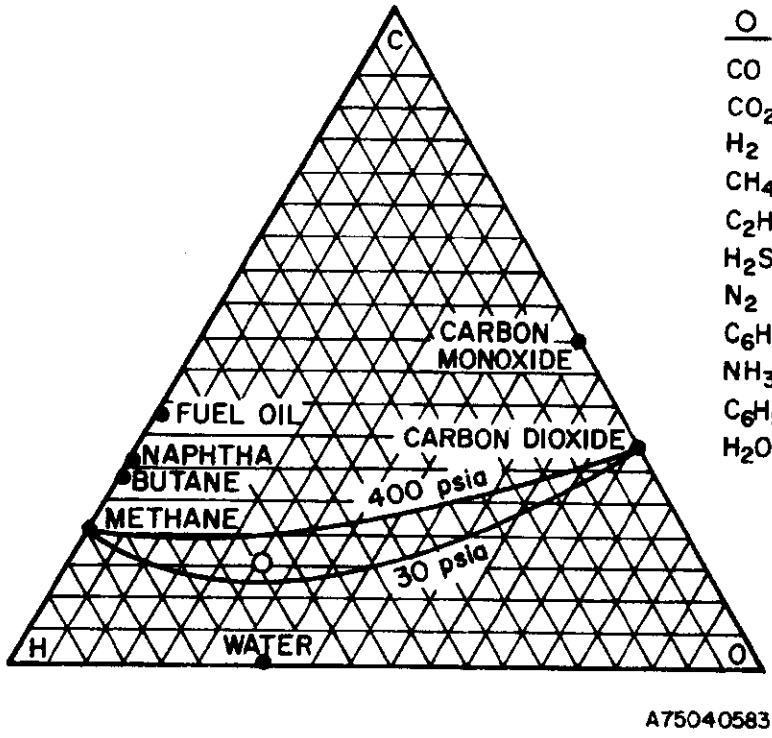

O	mol %
CO	19.8
CO_2	21.4
H_2	22.7
CH_4	22.54
C_2H_6	0.5
H_2S	1.4
N_2	1.1
C_6H_6	10.2
NH_3	0.3
C_6H_5OH	0.06
H_2O/GAS	1.31

Figure 79. EFFECT OF PRESSURE ON THE CARBON FORMATION AT 600°F

$$A + H_2S \rightleftarrows ES \quad (72)$$

$$ES + CO \rightleftarrows ES\text{-}CO \quad (73)$$

$$ES + H_2O \rightleftarrows ES\text{-}H_2O \quad (74)$$

$$ES\text{-}CO + ES\text{-}H_2O \rightleftarrows 2ES + H_2 + CO_2 \quad (75)$$

$$NH_3 + H_2S \rightleftarrows NH_4HS \quad (76)$$

$$2NH_3 + H_2S \rightleftarrows (NH_4)_2S \quad (77)$$

$$NH_4HS + nH_2O \rightleftarrows NH_4HS \cdot nH_2O \quad (78)$$

$$ES\text{-}CO + NH_3 \rightleftarrows X \quad (79)$$

$$ES\text{-}H_2O + NH_3 \rightleftarrows X \quad (80)$$

$$H_2S + X \rightleftarrows NH_4HS + ES \quad (81)$$

The catalysts used in this study are sulfur-active catalysts. The active sites become "effective" after being sulfided, as shown in Reaction 72. Hydrogen sulfide is used in this analysis, but carbon disulfide and carbonyl sulfide are equally effective. The reactants are adsorbed and products are formed as shown in Equations 73 through 75. The presence of ammonia causes several competing reactions: First, it competes with the active sites for sulfur (Reactions 76 and 77). Second, it ties up some of the steam needed to complete the water-gas shift reaction. Finally, it poisons the effective sites (Reactions 78 through 80). The poisoned sites are regenerated by the sulfur (Reaction 81) and eventually decomposed as the reverse reactions of Reactions 76 and 77.

Development of a Deactivation Rate Equation for Phenol Poisoning

The rate of deactivation due to phenol in the water-gas shift reaction can be represented graphically as shown in Figure 80. Experimental data, which were obtained at constant phenol concentrations and temperatures, are illustrated as circle points in Figure 80.

The rate-of-deactivation equation can be expressed in differential form —

$$-\left(\frac{\partial a}{\partial \theta}\right)_{C_{\phi OH}} = k a^{\beta} C_{\phi OH}^{\alpha} \quad (82)$$

where —

a = activity r/r_0

r = rate of the water-gas shift reaction at any time θ

r_o = initial rate of the water-gas shift reaction

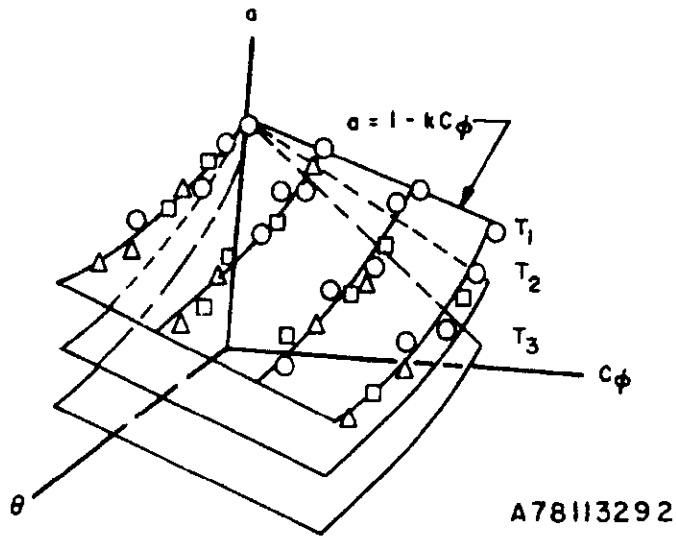

Figure 80. RATE OF DEACTIVATION DUE TO PHENOL AS A FUNCTION OF THE CONCENTRATION OF PHENOL AND TIME

θ = time, hours

k = rate constant

$C_{\phi OH}$ = concentration of phenol, mole fraction, wet basis

α, β = dimensionless exponents.

An adequate fit of the experimental data was obtained with $\beta = 1$, which leads to the integrated equation —

$$a = K \exp\left(-kC_{\phi OH}^{\alpha}\,\theta\right) \qquad (83)$$

Two independent fitting methods were used: a graphical solution and a least-squares fit utilizing a computer. These results are tabulated in Appendix D, and presented graphically in Figures 81 through 83. The final results obtained from these two methods were very similar and are presented in Table 16. The generalized rate-of-deactivation equation was developed based on the data obtained with the Shell Oil 538 and the Union Carbide UC-1870-46-1 catalysts. The data obtained with the Girdler (now the United Catalysts Inc.) G-93 catalyst, which were not used in the fit, were used to check the accuracy of the generalized rate-of-deactivation equation, and the results are presented in Figure 84. The average deviation of this check was 0.33% as compared with an average deviation of 0.19% for the fit of data obtained using the Shell Oil 538 and the Union Carbide UC-1870-46-1 catalysts. It is considered to be good.

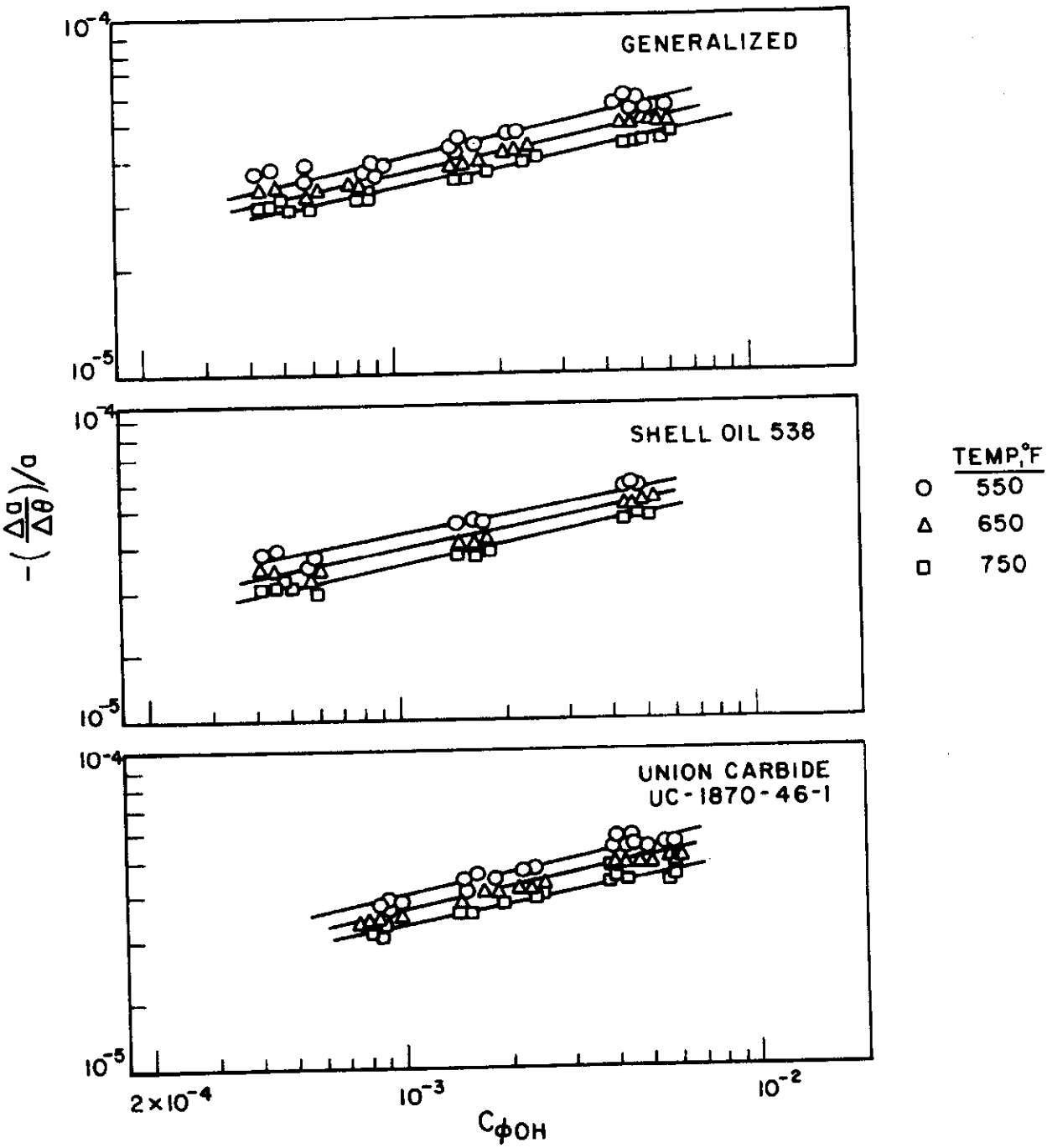

Figure 81. GRAPHICAL SOLUTION OF THE ORDER OF REACTION OF PHENOL

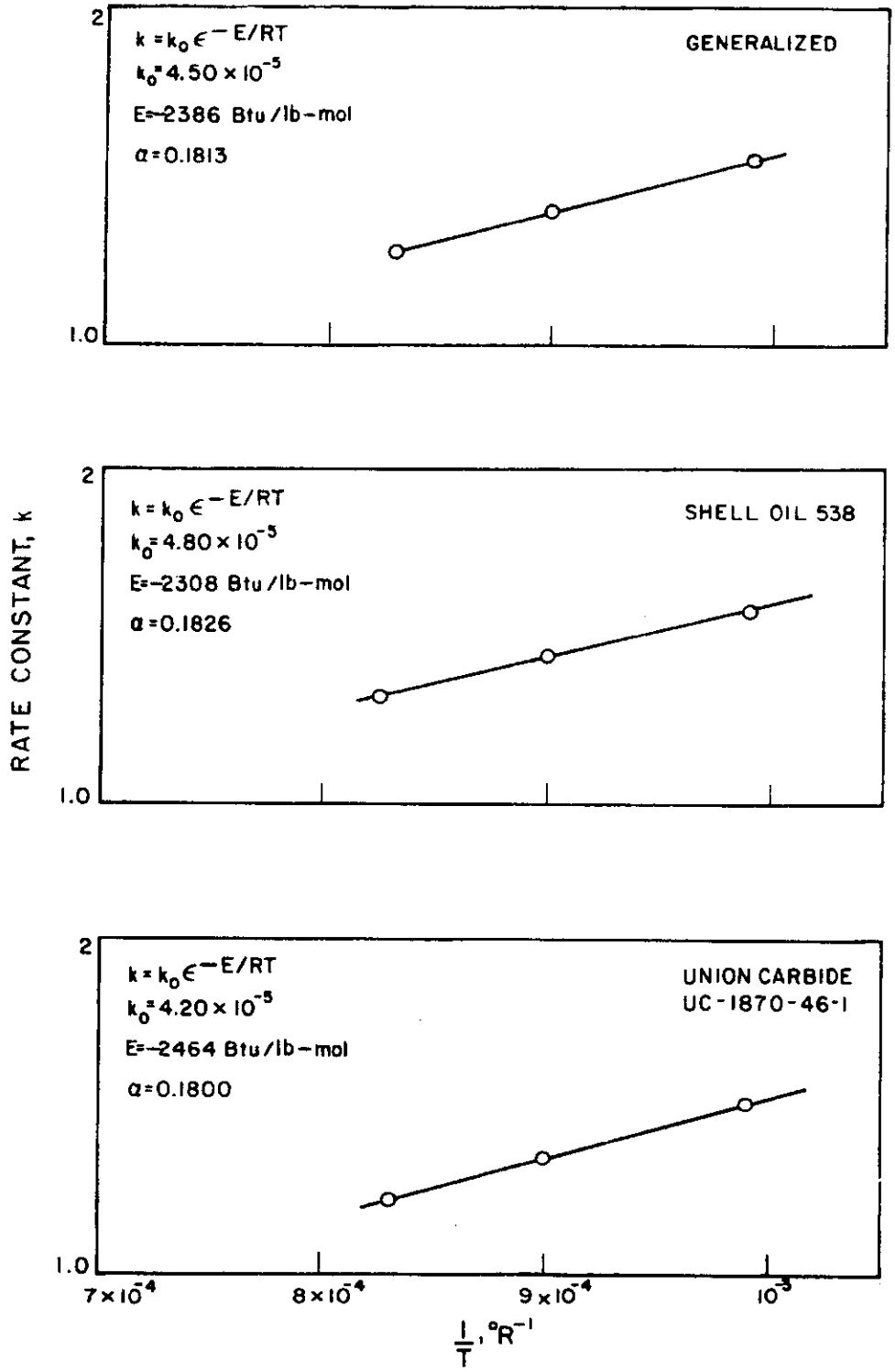

B78113297

Figure 82. ARRHENIUS PLOT FOR THE RATE OF DEACTIVATION DUE TO PHENOL

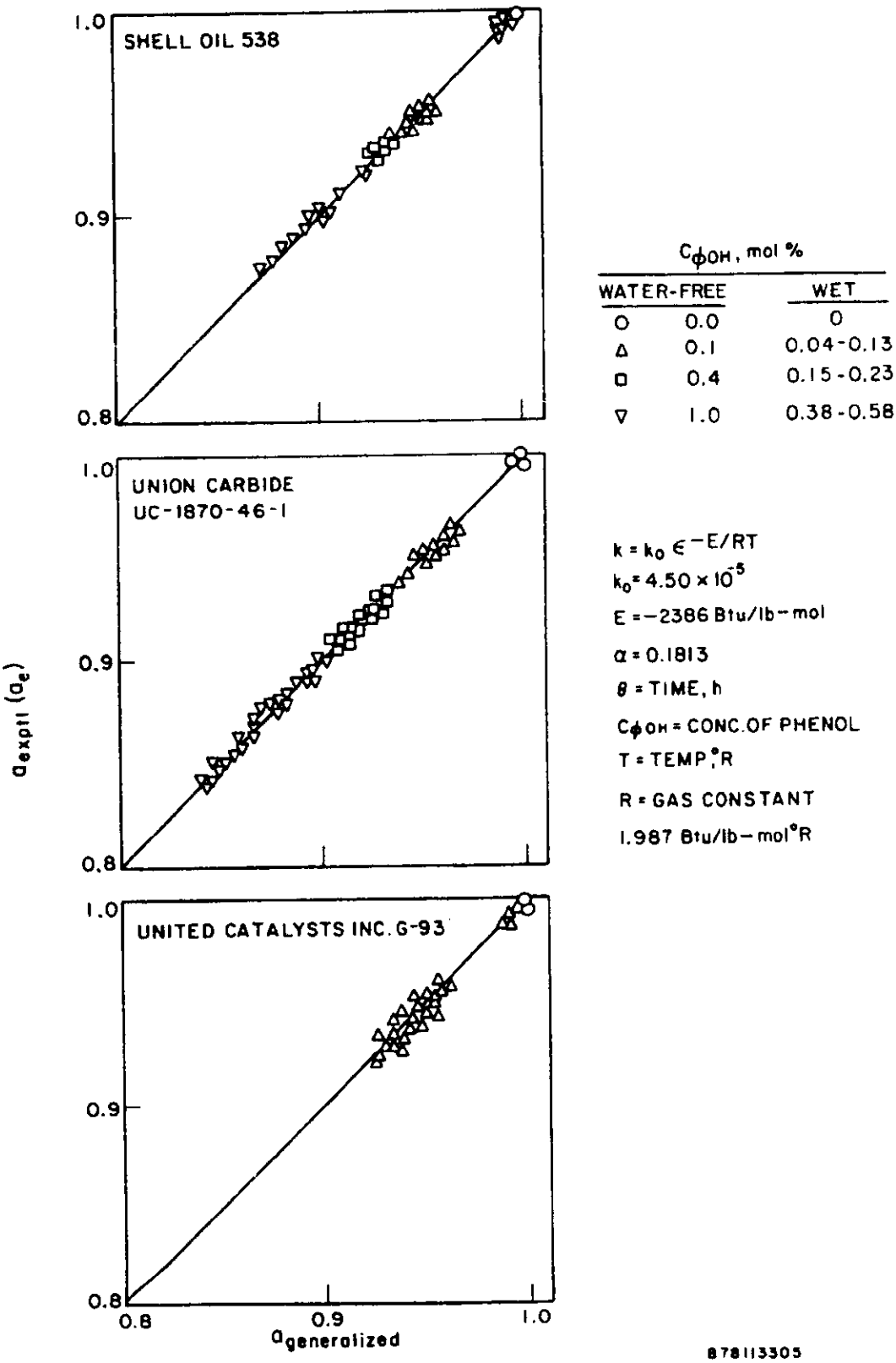

Figure 83. COMPARISON OF CALCULATED AND EXPERIMENTAL VALUES

Table 16. COMPARISON OF CONSTANTS IN THE RATE-OF-DEACTIVATION EQUATION

Catalyst	k_{oc}	k_{og}	E_c, Btu/lb-mol	E_g, Btu/lb-mol	α_c	α_g	$\Delta_{avg}{}^{c}$, %*	$\Delta_{avg}{}^{g}$, %
Shell	4.65×10^{-5}	4.80×10^{-5}	−2353	−2308	0.1862	0.1826	0.19	0.10
UC	4.23×10^{-5}	4.20×10^{-5}	−2445	−2464	0.1796	1.1800	0.14	0.56
G-93	--	--	--	--	--	--	0.33	0.26
General	4.44×10^{-5}	4.50×10^{-5}	−2399	−2386	0.1829	0.1813	0.20	0.35

* $\Delta_{avg} \equiv \dfrac{\left| \sum_{i}^{n} \Delta_i \right|}{n}$

c = computer fit by least squares.

g = graphical fit of data.

D78113323a

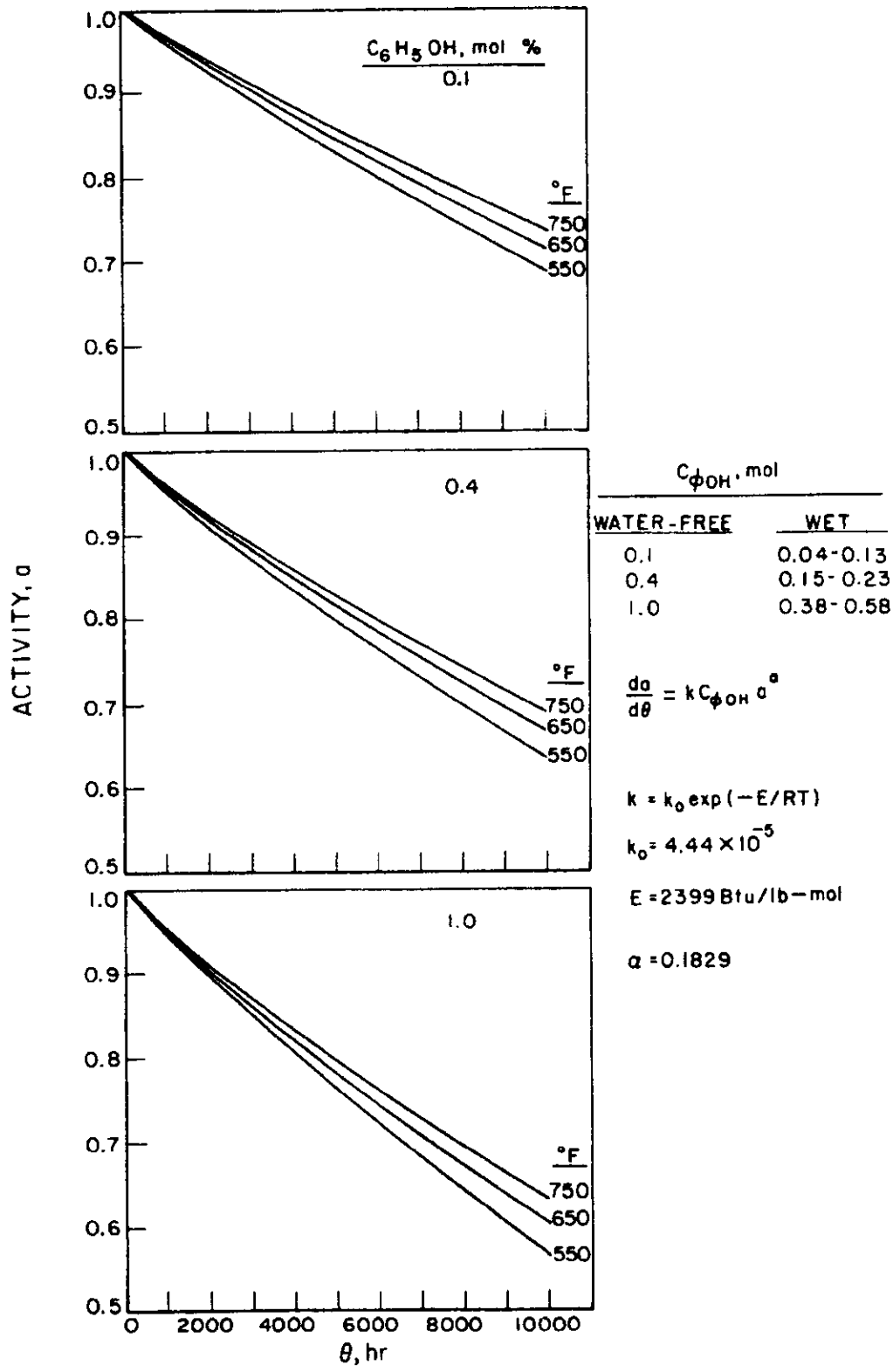

Figure 84. CALCULATED RATE-OF-DEACTIVATION VALUES

The final generalized rate-of-deactivation equation is —

$$-\left(\frac{da}{d\theta}\right) = kC_{\phi OH}^{0.1829}a \qquad (84)$$

or:

$$a = \exp\left(-kC_{\phi OH}^{0.1829}\,\theta\right) \qquad (85)$$

where —

$k = 4.44 \times 10^{-5} \exp(2399/RT)$

R = 1.987 Btu/lb mol-°R

T = temperature, °R .

Values calculated based on Equation 84 were compared with experimental data obtained using the Girdler G-93, Shell Oil 538, and Union Carbide UC-1870-46-1 catalysts, and the average deviation was 0.20%.